

Neutrino physics

M.C. Gonzalez-Garcia

Departament de Física Quàntica i Astrofísica and Institut de Ciències del Cosmos, Universitat de Barcelona, Barcelona, Spain,

Institució Catalana de Recerca i Estudis Avançats (ICREA), Barcelona, Spain,

C.N. Yang Institute for Theoretical Physics, Stony Brook University, Stony Brook, USA.

Abstract

The purpose of these lectures is to quantitatively summarize the present status of the phenomenology of massive neutrinos. In the first lecture I will present the low energy formalism for adding neutrino masses to the Standard Model and the induced leptonic mixing, and I will describe the status of the existing probes of the absolute neutrino mass scale. The second lecture is devoted to describing the phenomenology associated with neutrino flavour oscillations in vacuum and in matter and the corresponding experimental results observing these phenomena. In the third lecture I will present the minimal 3ν mixing picture emerging from the global description of the data. I will briefly comment on the status of extensions of this picture with additional light states and the possibility of non-standard neutrino interactions. I will also discuss some theoretical implications of these results, such as the existence of new physics, the estimate of the scale of this new physics, leptogenesis and collider signatures.

Keywords

Neutrinos, flavour oscillations, neutrino masses, sterile neutrinos, leptogenesis, lectures.

1 LECTURE I: Neutrino properties

1.1 Introduction

In 1930 Wolfgang Pauli postulated the existence of a new particle in order to reconcile the observed continuous spectrum of nuclear beta decay with energy conservation. The postulated particle had no electric charge and, in fact, Pauli himself pointed out that in order to do the job it had to weigh less than one percent of the proton mass, thus establishing the first limit on the *neutrino* mass. It was Fermi, who, in 1934 [1], gave its name to the neutrino and first proposed the four-fermion theory of beta decay. The neutrino was first observed by Cowan, Reines and collaborators [2] in 1956 in a reactor experiment. Soon after, in 1958 its helicity was determined by Goldhaber and collaborators [3] to be always -1 (*left-handed*) and as such were introduced in the Standard Model (SM).

Neutrinos are copiously produced in natural sources: in the burning of the stars, in the interaction of cosmic rays, in the Earth radioactivity... even as relics of the Big Bang. In the 1960's, neutrinos produced in the sun and in the atmosphere were first observed. In 1987, neutrinos from a supernova in the Large Magellanic Cloud were also detected. In 2013 the ICECUBE experiment detected high energy neutrinos from extragalactic sources. Neutrinos are also produced in *man-made* facilities, starting with the nuclear reactors which were the first source to be detected, and continuing with dedicated beams produced with particle accelerators. All these observations play an important role in understanding the properties of the neutrinos. In particular they allowed to establish that neutrinos carry *lepton flavour* characterizing them by the charged lepton with which they are produced in a SM weak current interaction.

The properties of the neutrino and in particular the question of its mass have intrigued physicists' minds ever since it was proposed. In the laboratory, neutrino masses have been kinematically searched

for without any positive result. Experiments achieved higher and higher precision, reaching upper limits for the electron-neutrino mass of 10^{-9} the proton mass, rather than the 10^{-2} originally obtained by Pauli. This raised the question of whether neutrinos are truly massless like photons.

It is clear that the answer to this question is limited by our capability of detecting the effect of a non-zero neutrino mass. This is a very difficult task in direct kinematic measurements. In 1957, however, Bruno Pontecorvo [4, 5] realized that the existence of neutrino masses may not only reveal itself in kinematic effects but it implies also the possibility of neutrino oscillations. Flavor oscillations of neutrinos were searched for using either neutrino beams from reactors or accelerators, or natural neutrinos generated at astrophysical sources (the Sun giving the largest flux) or in the atmosphere. The longer the distance that the neutrinos travel from their production point to the detector, the smaller masses that can be signaled by their oscillation. Indeed, the solar neutrinos allow us to search for masses that are as small as 10^{-5} eV, that is 10^{-14} of the proton mass!

Experiments studying natural neutrino fluxes were the first to provide us with strong evidence of neutrino masses and lepton flavour mixing. Experiments that measure the flux of atmospheric neutrinos found results that suggested the disappearance of muon-neutrinos when propagating over distances of order hundreds (or more) kilometers. Experiments that measured the flux of solar neutrinos found results that eventually demonstrated the disappearance of electron-neutrinos while propagating within the Sun. The disappearance of both atmospheric ν_μ 's and solar ν_e 's was most easily explained in terms of neutrino flavour transitions associated to neutrino masses and mixing. These results were tested and eventually confirmed with increasing precision in experiments using laboratory beams from nuclear reactors and accelerators. With the exception of a set of unconfirmed "hints" of possible eV scale mass states, all the oscillation signatures can be explained with the three flavor neutrinos (ν_e, ν_μ, ν_τ) expressed as quantum superposition of three massive states ν_i ($i = 1, 2, 3$) with different masses m_i .

In these lectures I first discuss some generic properties of the neutrinos related to the question of their mass and describe the low energy formalism for adding neutrino masses to the SM and the induced leptonic mixing. In the second lecture I describe the phenomenology associated with neutrino flavour oscillations in vacuum and transitions in matter and present the experimental evidence of neutrino oscillations. In the third lecture I will first present the derived values of neutrino masses and mixing when the bulk of data is consistently analyzed in the framework of mixing between the three active neutrinos. I will briefly comment on the status of extensions of this picture with additional light states and the possibility of non-standard neutrino interactions. I will also discuss some theoretical implications and some avenues open by these results: the existence of new physics, the estimate of the scale of this new physics, leptogenesis, collider signatures, etc. . .

In preparing these lectures, I have benefited from the many excellent books, such as Refs. [6–10], and several review articles. In the writing of these notes, I have used material from my review articles [11–13].

1.2 Standard Model of massless neutrinos

The Standard Model (SM) is based on the gauge group

$$G_{\text{SM}} = SU(3)_C \times SU(2)_L \times U(1)_Y, \quad (1)$$

with three fermion generations, where a single generation consists of five different representations of the gauge group,

$$Q_L(3, 2, \frac{1}{6}), U_R(3, 1, \frac{2}{3}), D_R(3, 1, -\frac{1}{3}), L_L(1, 2, -\frac{1}{2}), E_R(1, 1, -1). \quad (2)$$

where the numbers in parenthesis represent the corresponding charges under the group (1).

The model contains a single Higgs boson doublet, $\phi(1, 2, 1/2)$, whose vacuum expectation value breaks the gauge symmetry,

$$\langle \phi \rangle = \begin{pmatrix} 0 \\ \frac{v}{\sqrt{2}} \end{pmatrix} \implies G_{\text{SM}} \rightarrow SU(3)_C \times U(1)_{\text{EM}}. \quad (3)$$

Neutrinos are fermions that have neither strong nor electromagnetic interactions, *i.e.* they are singlets of $SU(3)_C \times U(1)_{\text{EM}}$. Active neutrinos have weak interactions, that is, they are not singlets of $SU(2)_L$. They reside in the lepton doublets L_L . Sterile neutrinos are define as having no SM gauge interactions, this is, they are singlets of the SM gauge group..

The SM has three active neutrinos accompanying the charged lepton mass eigenstates, e , μ and τ :

$$L_{L\ell} = \begin{pmatrix} \nu_{L\ell} \\ \ell_L^- \end{pmatrix}, \quad \ell = e, \mu, \tau. \quad (4)$$

Thus the charged current interaction terms for leptons read

$$- \mathcal{L}_{\text{CC}} = \frac{g}{\sqrt{2}} \sum_{\ell} \bar{\nu}_{L\ell} \gamma^{\mu} \ell_L^- W_{\mu}^+ + \text{h.c.} \quad (5)$$

In addition, the SM neutrinos have neutral current (NC) interactions,

$$- \mathcal{L}_{\text{NC}} = \frac{g}{2 \cos \theta_W} \sum_{\ell} \bar{\nu}_{L\ell} \gamma^{\mu} \nu_{L\ell} Z_{\mu}^0. \quad (6)$$

Equations (5) and (6) give all the neutrino interactions within the SM. In particular, Eq. (6) determines the decay width of the Z^0 boson into neutrinos which is proportional to the number of light left-handed neutrinos. At present the measurement of the invisible Z width yields $N_{\nu} = 2.984 \pm 0.008$ [14] making the existence of three, and only three, light (that is, $m_{\nu} \leq m_Z/2$) active neutrinos an experimental fact.

An important feature of the SM, which is relevant to the question of the neutrino mass is the fact that the SM with the gauge symmetry of Eq. (1) and the particle content of Eq. (2) presents an accidental global symmetry:

$$G_{\text{SM}}^{\text{global}} = U(1)_B \times U(1)_e \times U(1)_{\mu} \times U(1)_{\tau}. \quad (7)$$

$U(1)_B$ is the baryon number symmetry, and $U(1)_{e,\mu,\tau}$ are the three lepton flavor symmetries, with total lepton number given by $L = L_e + L_{\mu} + L_{\tau}$. It is an accidental symmetry because we do not impose it. It is a consequence of the gauge symmetry and the representations of the physical states.

In the SM fermion masses arise from the Yukawa interactions which couple a right-handed fermion with its left-handed doublet and the Higgs field (i, j are generation index),

$$- \mathcal{L}_{\text{Yukawa}} = Y_{ij}^d \bar{Q}_{Li} \phi D_{Rj} + Y_{ij}^u \bar{Q}_{Li} \tilde{\phi} U_{Rj} + Y_{ij}^{\ell} \bar{L}_{Li} \phi E_{Rj} + \text{h.c.}, \quad (8)$$

(where $\tilde{\phi} = i\tau_2 \phi^*$) and after spontaneous symmetry breaking generates a mass for fermions f

$$m_{ij}^f = Y_{ij}^f \frac{v}{\sqrt{2}}. \quad (9)$$

However, since no right-handed neutrinos exist in the model, the Yukawa interactions of Eq. (8) leave the neutrinos massless.

One may wonder if neutrino masses could arise from loop corrections or even by nonperturbative effects, however this cannot happen because any neutrino mass term that can be constructed with the SM fields would violate the total lepton symmetry, which, as mentioned above, is a global symmetry of the model so this is not allowed. I will return to this point in the last lecture.

It follows that the SM predicts that neutrinos are precisely massless. In order to add a mass to the neutrino the SM has to be extended.

1.3 Introducing massive neutrinos

As discussed above with the fermionic content and gauge symmetry of the SM one cannot construct a renormalizable mass term for the neutrinos. So in order to introduce a neutrino mass one must either extend the particle contents of the model or abandon gauge invariance and/or renormalizability. I will go back to this point in the last lecture.

Here I will assume that we want to keep the gauge symmetry and the renormalizability condition and we are going to explore the possibilities that we have to introduce a neutrino mass term if one adds to the SM an arbitrary number m of sterile neutrinos $\nu_{si}(1, 1, 0)$.

As we are going to see, related to the way we introduce the neutrino mass, it comes the fact that for the neutrino because it is the only neutral fermion, one can ask the question of whether a neutrino is a different particle than the antineutrino or they are both the same state.

If the neutrino is a different particle than the antineutrino we say that the neutrino is a *Dirac*-type particle, similar to any of the other charged fermions in the theory. Neutrino and antineutrino are then described by two different fields which involve two sets of creation-annihilation operators. If the neutrino and antineutrino are the same particle we say that the neutrino is a *Majorana*-type particle. This implies that there is only one field which describes both states and involves only one set of creation-annihilation operators. Mathematically this implies that it must be verified that:

$$\nu(x) = \nu^c(x) \quad (10)$$

Here ν^c indicates a charge conjugated field, $\nu^c \equiv C\bar{\nu}^T$ and C is the charge conjugation matrix. Notice that this condition implies that there is only one field which describes both neutrino and antineutrino states. Thus a Majorana neutrino can be described by a two-component spinor unlike the charged fermions, which are Dirac particles, and are represented by four-component spinors.

With the particle contents of the SM and the addition of an arbitrary m number of sterile neutrinos one can construct two types of mass terms that arise from *renormalizable* terms:

$$-\mathcal{L}_{M_\nu} = M_{Dij}\bar{\nu}_{si}\nu_{Lj} + \frac{1}{2}M_{Nij}\bar{\nu}_{si}\nu_{sj}^c + \text{h.c.} \quad (11)$$

M_D is a complex $m \times 3$ matrix and M_N is a symmetric matrix of dimension $m \times m$.

The first term is a Dirac mass term. It is generated after spontaneous electroweak symmetry breaking from Yukawa interactions

$$Y_{ij}^\nu \bar{\nu}_{si} \tilde{\phi}^\dagger L_{Lj} \Rightarrow M_{Dij} = Y_{ij}^\nu \frac{v}{\sqrt{2}} \quad (12)$$

similarly to the charged fermion masses. It conserves total lepton number but it breaks the lepton flavor number symmetries.

The second term in Eq. (11) is a Majorana mass term. It is different from the Dirac mass terms in many important aspects. It is a singlet of the SM gauge group. Therefore, it can appear as a bare mass term. Furthermore, since it involves two neutrino fields, it breaks lepton number by two units. More generally, such a term is allowed only if the neutrinos carry no additive conserved charge.

In general Eq. (11) can be rewritten as:

$$-\mathcal{L}_{M_\nu} = \frac{1}{2}\bar{\nu}^c M_\nu \vec{\nu} + \text{h.c.}, \quad (13)$$

where

$$M_\nu = \begin{pmatrix} 0 & M_D^T \\ M_D & M_N \end{pmatrix}, \quad (14)$$

and $\vec{\nu} = (\vec{\nu}_L, \vec{\nu}_s^c)^T$ is a $(3 + m)$ -dimensional vector. The matrix M_ν is complex and symmetric. It can be diagonalized by a unitary matrix of dimension $(3 + m)$, V^ν , so that

$$(V^\nu)^T M_\nu V^\nu = \text{diag}(m_1, m_2, \dots, m_{3+m}). \quad (15)$$

In terms of the resulting $3 + m$ mass eigenstates

$$\vec{\nu}_{\text{mass}} = (V^\nu)^\dagger \vec{\nu}, \quad (16)$$

Eq. (13) can be rewritten as:

$$-\mathcal{L}_{M_\nu} = \frac{1}{2} \sum_{k=1}^{3+m} m_k (\bar{\nu}_{\text{mass},k}^c \nu_{\text{mass},k} + \bar{\nu}_{\text{mass},k} \nu_{\text{mass},k}^c) = \frac{1}{2} \sum_{k=1}^{3+m} m_k \bar{\nu}_{Mk} \nu_{Mk}, \quad (17)$$

where

$$\nu_{Mk} = \nu_{\text{mass},k} + \nu_{\text{mass},k}^c = (V^{\nu\dagger} \vec{\nu})_k + (V^{\nu\dagger} \vec{\nu})_k^c \quad (18)$$

which clearly obey the Majorana condition Eq. (10).

From Eq. (18) we find that the weak-doublet components of the neutrino fields are:

$$\nu_{Li} = P_L \sum_{j=1}^{3+m} V_{ij}^\nu \nu_{Mj} \quad i = 1, 2, 3, \quad (19)$$

where P_L is the left-handed projector.

There are three interesting cases, differing in the hierarchy of scales between M_N and M_D :

(1) The scale of the mass eigenvalues of M_N is much higher than the scale of electroweak symmetry breaking $\langle \phi \rangle$. In this case the scale of the mass eigenvalues of M_N is much higher than the scale of electroweak symmetry breaking $\langle \phi \rangle$. The diagonalization of M_ν leads to three light, ν_l , and m heavy, N , neutrinos:

$$-\mathcal{L}_{M_\nu} = \frac{1}{2} \bar{\nu}_l M^l \nu_l + \frac{1}{2} \bar{N} M^h N \quad (20)$$

with

$$M^l \simeq -V_l^T M_D^T M_N^{-1} M_D V_l, \quad M^h \simeq V_h^T M_N V_h \quad (21)$$

and

$$V^\nu \simeq \begin{bmatrix} \left(1 - \frac{1}{2} M_D^\dagger M_N^{*-1} M_N^{-1} M_D\right) V_l & M_D^\dagger M_N^{*-1} V_h \\ -M_N^{-1} M_D V_l & \left(1 - \frac{1}{2} M_N^{-1} M_D M_D^\dagger M_N^{*-1}\right) V_h \end{bmatrix} \quad (22)$$

where V_l and V_h are 3×3 and $m \times m$ unitary matrices respectively. So the heavier are the heavy states, the lighter are the light ones. This is the *see-saw mechanism* [15–19]. Also, as seen from Eq. (22), the heavy states are mostly right-handed while the light ones are mostly left-handed. Both the light and the heavy neutrinos are Majorana particles. Two well-known examples of extensions of the SM leading to a see-saw mechanism for neutrino masses are SO(10) Grand Unified Theories [16, 17] and left-right symmetry [19]. In this case the SM is a good effective low energy theory.

(2) The scale of some eigenvalues of M_N is not higher than the electroweak scale. Now the SM is not even a good low energy effective theory: there are more than three light neutrinos, and they are mixtures of doublet and singlet fields. Again both light fields and the heavy ones are all of the Majorana-type.

(3) $M_N = 0$. This is equivalent to imposing lepton number symmetry on this model. Again, the SM is not even a good low energy theory: both the fermionic content and the assumed symmetries are different. Now only the first term in Eq. (11) is present, which is a Dirac mass term. It is generated by

the Higgs mechanism in the same way that charged fermions masses are generated. If indeed it is the only neutrino mass term present and $m = 3$, the six massive Majorana neutrinos combine to form three massive neutrino Dirac states, equivalently to the charged fermions. Technically in this particular case the 6×6 diagonalizing matrix in Eq. (15) is block diagonal and it can be written in terms of two 3×3 unitary matrices, here denoted by V^ν and V_R^ν , such that

$$V_R^{\nu\dagger} M_D V^\nu = \text{diag}(m_1, m_2, m_3). \quad (23)$$

So the neutrino mass term can be written as:

$$- \mathcal{L}_{M_\nu} = \sum_{k=1}^3 m_k \bar{\nu}_{Dk} \nu_{Dk} \quad (24)$$

where

$$\nu_{Dk} = (V^{\nu\dagger} \vec{\nu}_L)_k + (V_R^{\nu\dagger} \vec{\nu}_s)_k. \quad (25)$$

So in this we identify the three sterile neutrinos with the right handed component of a four-component spinor neutrino field while the weak-doublet components of the neutrino fields are

$$\nu_{Li} = P_L \sum_{j=1}^3 V_{ij}^\nu \nu_{Dj}, \quad i = 1, 2, 3. \quad (26)$$

As we will see the analysis of neutrino oscillations is the same whether the light neutrinos are of the Majorana- or Dirac-type. Only in the discussion of neutrinoless double beta decay the question of Majorana versus Dirac neutrinos is crucial.

1.4 Lepton mixing

The possibility of arbitrary mixing between two massive neutrino states was first introduced in Ref. [20]. In the general case general, we denote the neutrino mass eigenstates by $(\nu_1, \nu_2, \nu_3, \dots, \nu_n)$ where $n = 3 + m$, and the charged lepton mass eigenstates by (e, μ, τ) . The corresponding interaction eigenstates are denoted by (e^I, μ^I, τ^I) and $\vec{\nu} = (\nu_{Le}, \nu_{L\mu}, \nu_{L\tau}, \nu_{s1}, \dots, \nu_{sm})$. In the mass basis, leptonic charged current interactions are given by

$$- \mathcal{L}_{CC} = \frac{g}{\sqrt{2}} (\bar{e}_L \ \bar{\mu}_L \ \bar{\tau}_L) \gamma^\mu U \begin{pmatrix} \nu_1 \\ \nu_2 \\ \nu_3 \\ \cdot \\ \cdot \\ \nu_n \end{pmatrix} W_\mu^+ - \text{h.c.} \quad (27)$$

Here U is a $3 \times n$ matrix which verifies

$$UU^\dagger = I_{3 \times 3} \quad (28)$$

but in general $U^\dagger U \neq I_{n \times n}$.

Given the charged lepton mass matrix M_ℓ and the neutrino mass matrix M_ν in some interaction basis,

$$- \mathcal{L}_M = (\bar{e}_L^I \ \bar{\mu}_L^I \ \bar{\tau}_L^I) M_\ell \begin{pmatrix} e_R^I \\ \mu_R^I \\ \tau_R^I \end{pmatrix} + \frac{1}{2} \bar{\nu}^c M_\nu \vec{\nu} + \text{h.c.}, \quad (29)$$

we can find the diagonalizing matrices V^ℓ and V^ν :

$$V^{\ell\dagger} M_\ell M_\ell^\dagger V^\ell = \text{diag}(m_e^2, m_\mu^2, m_\tau^2), \quad V^{\nu\dagger} M_\nu^\dagger M_\nu V^\nu = \text{diag}(m_1^2, m_2^2, m_3^2, \dots, m_n^2). \quad (30)$$

Here V^ℓ is a unitary 3×3 matrix while V^ν the $n \times n$ unitary matrix in Eq. (15). The $3 \times n$ mixing matrix U can be found from these diagonalizing matrices:

$$U_{ij} = P_{\ell,ii} V_{ik}^{\ell\dagger} V_{kj}^\nu (P_{\nu,jj}). \quad (31)$$

P_ℓ is a diagonal 3×3 phase matrix, that is introduced to reduce by three the number of phases in U . P_ν is a diagonal matrix with additional arbitrary phases (chosen to reduce the number of phases in U) only for Dirac states. For Majorana neutrinos, this matrix is simply a unit matrix. The reason for that is that if one rotates a Majorana neutrino by a phase, this phase will appear in its mass term which will no longer be real. Thus, the number of phases that can be absorbed by redefining the mass eigenstates depends on whether the neutrinos are Dirac or Majorana particles. In particular, if there are only three Majorana neutrinos, U is a 3×3 matrix analogous to the Cabibbo-Kobayashi-Maskawa (CKM) matrix for the quarks [21, 22] but due to the Majorana nature of the neutrinos it depends on six independent parameters: three mixing angles and three phases. This is to be compared to the case of three Dirac neutrinos¹ where the number of physical phases is one, similarly to the CKM matrix. Note, however, that the two extra Majorana phases are very hard to measure since they are only physical if neutrino mass is non-zero and therefore the amplitude of any process involving them is suppressed a factor m_ν/E to some power where E is the energy involved in the process which is typically much larger than the neutrino mass. The most sensitive experimental probe of Majorana phases is the rate of neutrinoless $\beta\beta$ decay. If no new interactions for the charged leptons are present we can identify their interaction eigenstates with the corresponding mass eigenstates after phase redefinition. In this case the charged current lepton mixing matrix U is simply given by a $3 \times n$ sub-matrix of the unitary matrix V^ν . It is worth noticing that while for the case of 3 light Dirac neutrinos the procedure leads to a fully unitary U matrix for the light states, generically for three light Majorana neutrinos this is not the case when the full spectrum contains heavy neutrino states which have been integrated out as can be seen, from Eq. (22). However, as seen in Eq. (22), the unitarity violation is of the order $\mathcal{O}(M_D/M_N)$ and it is expected to be very small (at it is also severely constrained experimentally). Consequently in the analysis of oscillation data presented in next lectures the U matrix is assumed to be unitary.

1.5 Laboratory probes of ν mass scale and its nature

Kinematic constraints from weak decays

It was Fermi who first proposed a kinematic search for the neutrino mass from the hard part of the beta spectra in ${}^3\text{H}$ beta decay ${}^3\text{H} \rightarrow {}^3\text{He} + e^- + \bar{\nu}_e$. This is a superallowed transition, which means that the nuclear matrix elements do not generate any energy dependence, so that the electron spectrum is given by the phase space alone

$$\frac{dN}{dT} = C p E (Q - T) \sqrt{(Q - T)^2 - m_\nu^2} F(E). \quad (32)$$

where $E = T + m_e$, Q is the maximum energy and $F(E)$ is the Fermi function which incorporates final state Coulomb interactions.

Plotted in terms of the Kurie function $K(T) \equiv \sqrt{\frac{dN}{dT} \frac{1}{pEF(E)}}$ a non-vanishing neutrino mass m_ν provokes a distortion from the straight-line T -dependence at the end point: for $m_\nu = 0 \rightarrow T_{\max} = Q$ whereas for $m_\nu \neq 0 \rightarrow T_{\max} = Q - m_\nu$ as illustrated in Fig. 1. ${}^3\text{H}$ beta decay has a very small energy release $Q = 18.6 \text{ KeV}$ which makes it particularly sensitive to this kinematic effect. In the presence of mixing these limits have to be modified and in general they involve more than one flavor parameter. For neutrinos with small mass differences the distortion of the beta spectrum can be described by the single

¹In this case, as discussed above the 6×6 neutrino diagonalizing matrix is block diagonal and the V^ν in Eq. (31) is the 3×3 block introduced in Eq. (23).

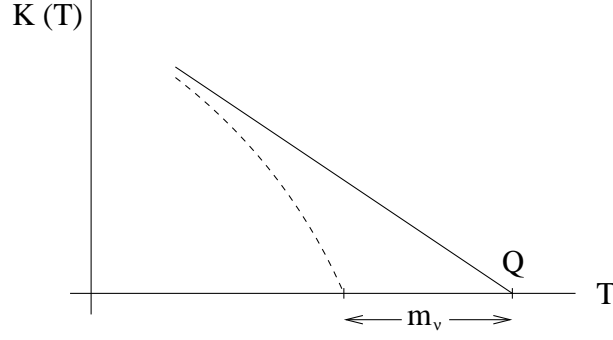


Fig. 1: Kinematic determination of m_ν

parameter substituting m_ν by

$$\left(m_{\nu_e}^{\text{eff}}\right)^2 = \sum_i m_i^2 |U_{ei}|^2 \quad (33)$$

The most recent result on the kinematic search for neutrino mass in tritium decay is from KATRIN [23], an experiment that so far has found no indication of $m_{\nu_e} \neq 0$ and sets an upper limit

$$m_{\nu_e}^{\text{eff}} < 1.1 \text{ eV}, \quad (34)$$

at 90% CL improving over the previous bound from the Mainz [24, 25] and Troitsk [26] experiments which constrained $m_{\nu_e}^{\text{eff}} < 2.2 \text{ eV}$ at 95% CL. KATRIN continues running with an estimated sensitivity limit of $m_{\nu_e}^{\text{eff}} \sim 0.2 \text{ eV}$.

For the other flavours the present limits are [14]

$$m_{\nu_\mu}^{\text{eff}} = \sqrt{\sum_i m_i^2 |U_{\mu i}|^2} < 190 \text{ keV} \quad (90\% \text{ CL}) \quad \text{from} \quad \pi^- \rightarrow \mu^- + \bar{\nu}_\mu \quad (35)$$

$$m_{\nu_\tau}^{\text{eff}} = \sqrt{\sum_i m_i^2 |U_{\tau i}|^2} < 18.2 \text{ MeV} \quad (95\% \text{ CL}) \quad \text{from} \quad \tau^- \rightarrow n\pi + \nu_\tau \quad (36)$$

Thus, in the presence of non-vanishing mixing the most stringent constraint on the absolute mass of any of the neutrinos is set by the limit from tritium beta decay in Eq. (34).

Dirac vs Majorana: neutrinoless double-beta decay

The most sensitive probe to whether neutrinos are Dirac or Majorana states is the neutrinoless double beta decay ($0\nu\beta\beta$):

$$(A, Z) \rightarrow (A, Z + 2) + e^- + e^-. \quad (37)$$

In the presence of neutrino masses and mixing the process in Eq.(37) can be generated at lower order in perturbation theory by the term represented by the diagram in Fig. 2 The amplitude of this process is proportional to the product of the two leptonic currents

$$M_{\alpha\beta} \propto [\bar{e}\gamma_\alpha(1 - \gamma_5)\nu_e] [\bar{e}\gamma_\beta(1 - \gamma_5)\nu_e] \propto \sum_i (U_{ei})^2 [\bar{e}\gamma_\alpha(1 - \gamma_5)\nu_i] [\bar{e}\gamma_\beta(1 - \gamma_5)\nu_i]. \quad (38)$$

The neutrino propagator in Fig. 2 can only arise from the contraction $\langle 0 | \nu_i(x)\nu_i(y)^T | 0 \rangle$. But if the neutrino is a Dirac particle ν_i field annihilates a neutrino states and creates an antineutrino state which are different, so the contraction $\langle 0 | \nu_i(x)\nu_i(y)^T | 0 \rangle = 0$ and $M_{\alpha\beta} = 0$. On the other hand, if ν_i is a Majorana particle, neutrino and antineutrino are described by the same field and $\langle 0 | \nu_i(x)\nu_i(y)^T | 0 \rangle \neq 0$.

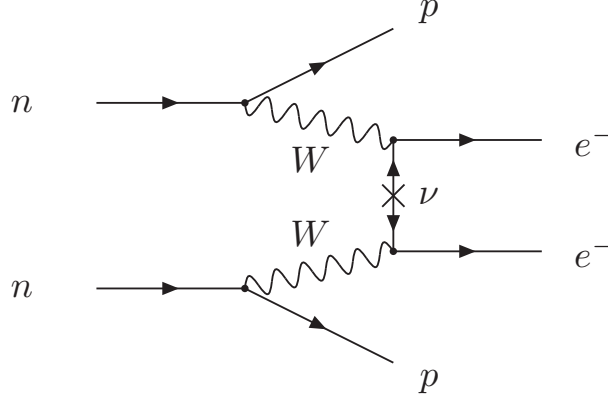


Fig. 2: Feynman diagram for neutrinoless double-beta decay.

The conclusion is that in order to induce the $0\nu\beta\beta$ decay, neutrinos must be Majorana particles. This is consistent with the fact that the process (37) violates total lepton number by two units. Conversely, if $0\nu\beta\beta$ decay is observed, massive neutrinos cannot be exact Dirac states [27].

After some algebra one finds that the rate of the process is proportional to the *effective Majorana mass of ν_e* ,

$$m_{ee} = \left| \sum_i m_i U_{ei}^2 \right| \quad (39)$$

which, in addition to the masses and mixing parameters that affect the tritium beta decay spectrum, depends also on the leptonic CP violating phases.

The observable determined by the experiments is the half-life of the decay. Under the assumption that the Majorana neutrino mass is the only source of lepton number violation at low energies, the decay half-life is given by:

$$(T_{1/2}^{0\nu})^{-1} = G^{0\nu} |M^{0\nu}|^2 \left(\frac{m_{ee}}{m_e} \right)^2, \quad (40)$$

where $G^{0\nu}$ is the phase space integral taking into account the final atomic state, and $|M^{0\nu}|$ is the nuclear matrix element of the transition.

At present the strongest bound on $0\nu\beta\beta$ decay lifetime comes from the search in KamLAND-Zen experiment [28] which uses 13 Tons of Xe-loaded liquid scintillator to search for the decay $0\nu\beta\beta$ of ^{136}Xe and has set a bound on the half-life of $T_{1/2}^{0\nu} > 1.07 \times 10^{26}$ yr at 90% CL. From Eq. (40) we see that nuclear structure details enter relation between the decay rate (or lifetime) and the effective Majorana mass. As a consequence uncertainties in the nuclear structure calculations result in a spread of m_{ee} values for a given $T_{1/2}^{0\nu}$ by a factor of 2–3 [29]. Using a variety of nuclear matrix element calculations, the corresponding upper bound on the effective Majorana mass is

$$m_{ee} < 61 - 165 \text{ meV}. \quad (41)$$

This bound is stronger than the one from tritium beta decay but it is model dependent because it requires that neutrinos are Majorana particles and that their mass is the only source of lepton number violation generating neutrinoless double beta decay.

Cosmological bounds

Neutrinos, like any other particles, contribute to the total energy density of the Universe. Furthermore light neutrinos are relativist through most of the evolution of the Universe. As a consequence they can

play a relevant role in large scale structure formation and leave clear signatures in several cosmological observables.

Within what we presently know of their masses, neutrinos are relativistic through most of the evolution of the Universe and being very weakly interacting they decoupled early in cosmic history. Depending on their exact masses they can impact the cosmic microwave background spectra, in particular by altering the value of the redshift for matter-radiation equality. More importantly, their free streaming suppresses the growth of structures on scales smaller than the horizon at the time when they become non-relativistic and therefore affects the matter power spectrum which is probed from surveys of the Large Scale Structure distribution. Because of these effects it is possible to infer constraints, although indirect, on the neutrino masses by comparing the most recent cosmological data with the current theoretical predictions.

The relevant quantity in these studies is the total neutrino energy density in our Universe, $\Omega_\nu h^2$ (where h is the Hubble constant normalized to $H_0 = 100 \text{ km s}^{-1} \text{ Mpc}^{-1}$). At present $\Omega_\nu h^2$ is related to the total mass in the form of neutrinos

$$\Omega_\nu h^2 = \sum_i m_i / (94 \text{ eV}) . \quad (42)$$

Therefore cosmological data gives information on the sum of the neutrino masses and has very little to say on their mixing.

Because of these effects, the recent precise astrophysical and cosmological observations can provide indirect upper limits on absolute neutrino masses competitive with those from laboratory experiments. At present the most robust bounds come from the analysis of Planck results which within the Λ -Cold-Dark-Matter model imply $\sum_i m_i \leq 0.17 - 0.74 \text{ eV}$ where the range includes variations of the data sets included in the analysis. One must always keep in mind that these bounds apply *within a given cosmological model* and consequently variations of the model can relax the bounds.

1.6 Summary

In the SM neutrinos are purely left-handed and strictly massless. Neutrino masses can be introduced in the model at the expense of adding new right-handed – hence sterile – states, and/or breaking total lepton number. Depending on the way the mass term is introduced, the massive neutrinos are Dirac particles, as any other fermions of the SM for which neutrinos and antineutrinos are different states, or Majorana particles, being their own antiparticles. In this second case one may gain an understanding of why neutrino masses are smaller than other fermion masses. Massive neutrinos open up the possibility of flavour mixing and CP violation in the lepton sector similar to the quark sector. So far direct searches for neutrino masses have result only into limits, the strongest model independent bound is $\sim \text{eV}$ from tritium β decay.

2 LECTURE II: Flavour oscillations

2.1 Mass-induced flavour oscillations in vacuum

If neutrinos have masses and lepton flavours are mixed in the weak CC interactions, lepton flavour is not conserved in neutrino propagation [4,5]. This phenomenon is usually referred to as *neutrino oscillations*. In brief, a weak eigenstates, ν_α , which by default is the state produced in the weak CC interaction of a charged lepton ℓ_α , is the linear combination determined by the mixing matrix U

$$|\nu_\alpha\rangle = \sum_{i=1}^n U_{\alpha i}^* |\nu_i\rangle, \quad (43)$$

where ν_i are the mass eigenstates and here n is the number of light neutrino species (implicit in our definition of the state $|\nu\rangle$ is its energy-momentum and space-time dependence). After traveling a distance L ($L \simeq ct$ for relativistic neutrinos), that state evolves as:

$$|\nu_\alpha(t)\rangle = \sum_{i=1}^n U_{\alpha i}^* |\nu_i(t)\rangle. \quad (44)$$

This neutrino can then undergo a charged-current (CC) interaction producing a charge lepton ℓ_β , $\nu_\alpha(t)N' \rightarrow \ell_\beta N$, with a probability

$$P_{\alpha\beta} = |\langle \nu_\beta | \nu_\alpha(t) \rangle|^2 = \left| \sum_{i=1}^n \sum_{j=1}^n U_{\alpha i}^* U_{\beta j} \langle \nu_j | \nu_i(t) \rangle \right|^2. \quad (45)$$

Assuming that $|\nu\rangle$ is a plane wave, $|\nu_i(t)\rangle = e^{-iE_i t} |\nu_i(0)\rangle$,² with $E_i = \sqrt{p_i^2 + m_i^2}$ and m_i being, respectively, the energy and the mass of the neutrino mass eigenstate ν_i . In all practical cases neutrinos are very relativistic, so $p_i \simeq p_j \equiv p \simeq E$. We can then write

$$E_i = \sqrt{p_i^2 + m_i^2} \simeq p + \frac{m_i^2}{2E}, \quad (46)$$

and use the orthogonality of the mass eigenstates, $\langle \nu_j | \nu_i \rangle = \delta_{ij}$, to arrive to the following form for $P_{\alpha\beta}$:

$$P_{\alpha\beta} = \delta_{\alpha\beta} - 4 \sum_{i<j}^n \text{Re}[U_{\alpha i} U_{\beta i}^* U_{\alpha j}^* U_{\beta j}] \sin^2 X_{ij} + 2 \sum_{i<j}^n \text{Im}[U_{\alpha i} U_{\beta i}^* U_{\alpha j}^* U_{\beta j}] \sin 2X_{ij}, \quad (47)$$

where

$$X_{ij} = \frac{(m_i^2 - m_j^2)L}{4E} = 1.267 \frac{\Delta m_{ij}^2}{\text{eV}^2} \frac{L/E}{\text{m/MeV}}. \quad (48)$$

If we had made the same derivation for antineutrino states we would have ended with a similar expression but with the exchange $U \rightarrow U^*$. Consequently we conclude that the first term in the right-hand-side of Eq. (47) is CP conserving since it is the same for neutrinos and antineutrinos, while the last one is CP violating because it has opposite sign for neutrinos and antineutrinos.

Equation (47) oscillates in distance with oscillation lengths

$$L_{0,ij}^{\text{osc}} = \frac{4\pi E}{|\Delta m_{ij}^2|}, \quad (49)$$

²For a pedagogical discussion of the quantum mechanical description of flavour oscillations in the wave package approach see for example Ref. [8]. A recent review of the quantum mechanical aspects and subtleties on neutrino oscillations can be found in Ref. [30].

and with amplitudes proportional to products of elements in the mixing matrix. Thus, neutrinos must have different masses ($\Delta m_{ij}^2 \neq 0$) and they must have not vanishing mixing ($U_{\alpha i} U_{\beta i} \neq 0$) in order to undergo flavour oscillations. Also, from Eq.(47) we see that the Majorana phases cancel out in the oscillation probability. This is expected because flavour oscillation is a total lepton number conserving process.

Ideally, a neutrino oscillation experiment would like to measure an oscillation probability over a distance L between the source and the detector, for neutrinos of a definite energy E . In practice, neutrino beams, both from natural or artificial sources, are never monoenergetic, but have an energy spectrum $\Phi(E)$. In addition each detector has a finite energy resolution. Under these circumstances what is measured is an average probability

$$\begin{aligned} \langle P_{\alpha\beta} \rangle &= \frac{\int dE \frac{d\Phi}{dE} \sigma(E) P_{\alpha\beta}(E) \epsilon(E)}{\int dE \frac{d\Phi}{dE} \sigma_{CC}(E) \epsilon(E)} \\ &= \delta_{\alpha\beta} - 4 \sum_{i<j}^n \text{Re}[U_{\alpha i} U_{\beta i}^* U_{\alpha j}^* U_{\beta j}] \langle \sin^2 X_{ij} \rangle + 2 \sum_{i<j}^n \text{Im}[U_{\alpha i} U_{\beta i}^* U_{\alpha j}^* U_{\beta j}] \langle \sin 2X_{ij} \rangle. \end{aligned} \quad (50)$$

σ is the cross section for the process in which the neutrino flavour is detected, and $\epsilon(E)$ is the detection efficiency. The minimal range of the energy integral is determined by the energy resolution of the experiment.

It is clear from the above expression that if $(E/L) \gg |\Delta m_{ij}^2|$ ($L \ll L_{0,ij}^{\text{osc}}$) so $\sin^2 X_{ij} \ll 1$, the oscillation phase does not give any appreciable effect. Conversely if $L \gg L_{0,ij}^{\text{osc}}$, many oscillation cycles occur between production and detection so the oscillating term is averaged to $\langle \sin^2 X_{ij} \rangle = 1/2$.

We summarize in Table 1. the typical values of L/E for different types of neutrino sources and experiments and the corresponding ranges of Δm^2 to which they can be most sensitive.

Table 1: Characteristic values of L and E for experiments performed using various neutrino sources and the corresponding ranges of $|\Delta m^2|$ to which they can be most sensitive to flavour oscillations in vacuum. SBL stands for short baseline and LBL for long baseline.

Experiment		L (m)	E (MeV)	$ \Delta m^2 $ (eV ²)
Solar		10^{10}	1	10^{-10}
Atmospheric		$10^4 - 10^7$	$10^2 - 10^5$	$10^{-1} - 10^{-4}$
Reactor	SBL	$10^2 - 10^3$	1	$10^{-2} - 10^{-3}$
	LBL	$10^4 - 10^5$		$10^{-4} - 10^{-5}$
Accelerator	SBL	10^2	$10^3 - 10^4$	> 0.1
	LBL	$10^5 - 10^6$	$10^3 - 10^4$	$10^{-2} - 10^{-3}$

Historically, the results of neutrino oscillation experiments were interpreted assuming two-neutrino states so there is only one oscillating phase, the mixing matrix depends on a single mixing angle θ and no CP violation effect in oscillations is possible. At present, as we will discuss in the third lecture we need at least the mixing among three-neutrino states to fully describe the bulk of experimental results. However, in many cases, the observed results can be understood in terms of oscillations dominantly driven by one Δm^2 . In this limit $P_{\alpha\beta}$ of Eq.(47) takes the form [5]

$$P_{\alpha\beta} = \delta_{\alpha\beta} - (2\delta_{\alpha\beta} - 1) \sin^2 2\theta \sin^2 X. \quad (51)$$

In this effective $2 - \nu$ limit, changing the sign of the mass difference, $\Delta m^2 \rightarrow -\Delta m^2$, and changing the octant of the mixing angle, $\theta \rightarrow \frac{\pi}{2} - \theta$, is just redefining the mass eigenstates, $\nu_1 \leftrightarrow \nu_2$: $P_{\alpha\beta}$ must be invariant under such transformation. So the physical parameter space can be covered with either $\Delta m^2 \geq 0$ with $0 \leq \theta \leq \frac{\pi}{2}$, or, alternatively, $0 \leq \theta \leq \frac{\pi}{4}$ with either sign for Δm^2 .

However, from Eq. (51) we see that $P_{\alpha\beta}$ is actually invariant under the change of sign of the mass splitting *and* the change of octant of the mixing angle separately. This implies that there is a two-fold discrete ambiguity since the two different sets of physical parameters, $(\Delta m^2, \theta)$ and $(\Delta m^2, \frac{\pi}{2} - \theta)$, give the same transition probability in vacuum. In other words, one could not tell from a measurement of, say, $P_{e\mu}$ in vacuum whether the larger component of ν_e resides in the heavier or in the lighter neutrino mass eigenstate. This symmetry is broken when one considers mixing of three or more neutrinos in the flavour evolution and/or when the neutrinos traverse regions of dense matter as we describe in the following.

2.2 Propagation of massive neutrinos in matter

When neutrinos propagate in dense matter, the interactions with the medium affect their properties. These effects are either coherent or incoherent. For purely incoherent inelastic ν -p scattering, the characteristic cross section is very small:

$$\sigma \sim \frac{G_F^2 s}{\pi} \sim 10^{-43} \text{cm}^2 \left(\frac{E}{1 \text{ MeV}} \right)^2 . \quad (52)$$

The smallness of this cross section is demonstrated by the fact that if a beam of 10^{10} neutrinos with $E \sim 1 \text{ MeV}$ was aimed at the Earth, only one would be deflected by the Earth matter. It may seem then that for neutrinos matter is irrelevant. However, one must take into account that Eq. (52) does not contain the contribution from forward elastic coherent interactions. In coherent interactions, the medium remains unchanged and it is possible to have interference of scattered and unscattered neutrino waves which enhances the effect. Coherence further allows one to decouple the evolution equation of the neutrinos from the equations of the medium. In this approximation, the effect of the medium is described by an effective potential which depends on the density and composition of the matter [31].

For example the effective potential for the evolution of ν_e in a medium with electrons, protons and neutrons due to its CC interactions is given by (a detailed derivation of this result can be found, for instance, in Refs. [8, 11, 12])

$$V_C = \sqrt{2} G_F N_e . \quad (53)$$

where N_e is the electron number density. For $\bar{\nu}_e$ the sign of V_C is reversed. This potential can also be expressed in terms of the matter density ρ :

$$V_C = \sqrt{2} G_F N_e \simeq 7.6 Y_e \frac{\rho}{10^{14} \text{g/cm}^3} \text{ eV} , \quad (54)$$

where $Y_e = \frac{N_e}{N_p + N_n}$ is the relative number density. Three examples that are relevant to observations are the following:

- At the Earth core $\rho \sim 10 \text{ g/cm}^3$ and $V_C \sim 10^{-13} \text{ eV}$;
- At the solar core $\rho \sim 100 \text{ g/cm}^3$ and $V_C \sim 10^{-12} \text{ eV}$

In the same way we can obtain the effective potentials for any flavour neutrino or antineutrino due to interactions with different particles in the medium. For ν_μ and ν_τ , $V_C = 0$ for most media while for any active neutrino the effective potential due to NC interactions in neutral medium is $V_N = -1/\sqrt{2} G_F N_n$ where N_n is the number density of neutrons.

There are several derivations in the literature of the evolution equation of a neutrino system in matter (see, for instance, Refs. [32–34]). In here we start by considering a state which is an admixture of two neutrino species $|\nu_\alpha\rangle$ and $|\nu_\beta\rangle$ or, equivalently, of $|\nu_1\rangle$ and $|\nu_2\rangle$:

$$|\Phi(x)\rangle = \Phi_\alpha(x)|\nu_\alpha\rangle + \Phi_\beta(x)|\nu_\beta\rangle = \Phi_1(x)|\nu_1\rangle + \Phi_2(x)|\nu_2\rangle \quad (55)$$

We decompose the neutrino wave function: $\Phi_i(x) = \nu_i(x)\phi_i(x)$ where $\phi_i(x)$ is the spinor part.

The evolution of Φ in a medium is described by a system of coupled Dirac equations, but after several approximations the spinorial part can be drop out and we end up with an equation which can be

written in matrix form as [31]:

$$-i \frac{\partial}{\partial x} \begin{pmatrix} \nu_\alpha \\ \nu_\beta \end{pmatrix} = \left(-\frac{M_w^2}{2E} \right) \begin{pmatrix} \nu_\alpha \\ \nu_\beta \end{pmatrix}, \quad (56)$$

where we have defined an effective mass matrix in matter:

$$M_w^2 = \begin{pmatrix} \frac{m_1^2 + m_2^2}{2} + 2EV_\alpha - \frac{\Delta m^2}{2} \cos 2\theta & \frac{\Delta m^2}{2} \sin 2\theta \\ \frac{\Delta m^2}{2} \sin 2\theta & \frac{m_1^2 + m_2^2}{2} + 2EV_\beta + \frac{\Delta m^2}{2} \cos 2\theta \end{pmatrix}. \quad (57)$$

Here $\Delta m^2 = m_2^2 - m_1^2$.

We define the instantaneous mass eigenstates in matter, ν_i^m , as the eigenstates of M_w for a fixed value of x (or t). They are related to the interaction eigenstates through a unitary rotation,

$$\begin{pmatrix} \nu_\alpha \\ \nu_\beta \end{pmatrix} = U(\theta_m) \begin{pmatrix} \nu_1^m \\ \nu_2^m \end{pmatrix} = \begin{pmatrix} \cos \theta_m & \sin \theta_m \\ -\sin \theta_m & \cos \theta_m \end{pmatrix} \begin{pmatrix} \nu_1^m \\ \nu_2^m \end{pmatrix}. \quad (58)$$

The eigenvalues of M_w , that is, the effective masses in matter are given by [31, 35]:

$$\mu_{1,2}^2(x) = \frac{m_1^2 + m_2^2}{2} + E(V_\alpha + V_\beta) \mp \frac{1}{2} \sqrt{(\Delta m^2 \cos 2\theta - A)^2 + (\Delta m^2 \sin 2\theta)^2}, \quad (59)$$

while the mixing angle in matter is given by

$$\tan 2\theta_m = \frac{\Delta m^2 \sin 2\theta}{\Delta m^2 \cos 2\theta - A}. \quad (60)$$

The quantity A is defined by

$$A \equiv 2E(V_\alpha - V_\beta). \quad (61)$$

In Fig. 3 we plot the effective masses and the mixing angle in matter as functions of the potential A , for $A > 0$ and $\Delta m^2 \cos 2\theta > 0$. Notice that even massless neutrinos acquire non-vanishing effective masses in matter. Also the sign of A depends on the composition of the medium and on the flavour composition of the neutrino state considered. From the expressions above we see that for a given sign of A the mixing angle in matter is larger(smaller) than in vacuum if this last one is in the first (second) octant. Therefore the symmetry about 45 degrees which existing in vacuum oscillations between two neutrino states is broken by the matter potential in propagation in a medium.

The expressions above show that very important effects are present when A , is close to $\Delta m^2 \cos 2\theta$. In particular, as seen in Eq. (60), the tangent of the mixing angle changes sign if, along its path, the neutrino passes by some matter density region satisfying, for its energy, the *resonance condition*

$$A_R = \Delta m^2 \cos 2\theta. \quad (62)$$

This implies that if the neutrino is created in a region where the relevant potential satisfies $A_0 > A_R$ (A_0 here is the value of the relevant potential at the production point), then the effective mixing angle in matter at the production point is such that $\text{sgn}(\cos 2\theta_{m,0}) = -\text{sgn}(\cos 2\theta)$. So the flavour component of the mass eigenstates is inverted as compared to their composition in vacuum. In particular, if at production point we have $A_0 = 2A_R$, then $\theta_{m,0} = \frac{\pi}{2} - \theta$. Asymptotically, for $A_0 \gg A_R$, $\theta_{m,0} \rightarrow \frac{\pi}{2}$. In other words, if in vacuum the lightest (heaviest) mass eigenstate has a larger projection on the flavour α (β), inside a matter with density and composition such that $A > A_R$, the opposite holds. So if the neutrino system is traveling across a monotonically varying matter potential, the dominant flavour component of a given mass eigenstate changes when crossing the region with $A = A_R$. This phenomenon is known as *level crossing*.

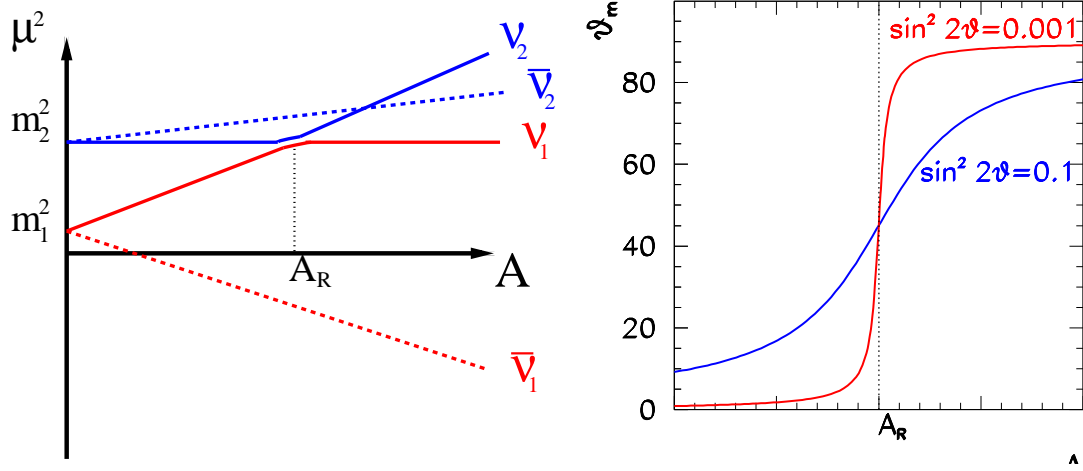


Fig. 3: Effective masses (left) and mixing(right) acquired in the medium by a system of two massive neutrinos as a function of the potential A [see Eq. (59)].

From the expression above we see that the oscillation length in matter,

$$L^{\text{osc}} = \frac{L_0^{\text{osc}} \Delta m^2}{\sqrt{(\Delta m^2 \cos 2\theta - A)^2 + (\Delta m^2 \sin 2\theta)^2}}, \quad (63)$$

where the oscillation length in vacuum, L_0^{osc} , was defined in Eq. (49), presents a resonant behaviour. At the resonance point the oscillation length is

$$L_R^{\text{osc}} = \frac{L_0^{\text{osc}}}{\sin 2\theta}. \quad (64)$$

The width (in distance) of the resonance, δr_R , corresponding to $\delta A_R = 2\Delta m^2 \sin^2 2\theta$ is

$$\delta r_R = \frac{\delta A_R}{\left| \frac{dA}{dr} \right|_R} \quad (65)$$

For constant A , *i.e.*, for constant matter density, the evolution of the neutrino system is described just in terms of the masses and mixing in matter. But for varying A , this is in general not the case.

In the general case, taking the time derivative of Eq. (58), we find:

$$\frac{\partial}{\partial t} \begin{pmatrix} \nu_\alpha \\ \nu_\beta \end{pmatrix} = \dot{U}(\theta_m) \begin{pmatrix} \nu_1^m \\ \nu_2^m \end{pmatrix} + U(\theta_m) \begin{pmatrix} \dot{\nu}_1^m \\ \dot{\nu}_2^m \end{pmatrix}. \quad (66)$$

Using the evolution equation in the flavor basis, Eq. (56), we get

$$i \begin{pmatrix} \dot{\nu}_1^m \\ \dot{\nu}_2^m \end{pmatrix} = \frac{1}{2E} U^\dagger(\theta_m) M_w^2 U(\theta_m) \begin{pmatrix} \nu_1^m \\ \nu_2^m \end{pmatrix} - i U^\dagger \dot{U}(\theta_m) \begin{pmatrix} \nu_1^m \\ \nu_2^m \end{pmatrix}. \quad (67)$$

For constant matter density, θ_m is constant and the second term vanishes. In general, using the definition of the effective masses $\mu_i(t)$ in Eq. (59), and subtracting a diagonal piece $(\mu_1^2 + \mu_2^2)/2E \times I$, we can rewrite the evolution equation as:

$$i \begin{pmatrix} \dot{\nu}_1^m \\ \dot{\nu}_2^m \end{pmatrix} = \frac{1}{4E} \begin{pmatrix} -\Delta(t) & -4iE\dot{\theta}_m(t) \\ 4iE\dot{\theta}_m(t) & \Delta(t) \end{pmatrix} \begin{pmatrix} \nu_1^m \\ \nu_2^m \end{pmatrix} \quad (68)$$

where we defined $\Delta(t) \equiv \mu_2^2(t) - \mu_1^2(t)$.

The evolution equations, Eq. (68), constitute a system of coupled equations: the instantaneous mass eigenstates, ν_i^m , mix in the evolution and are not energy eigenstates. The importance of this effect is controlled by the relative size of the off-diagonal piece $4E\dot{\theta}_m(t)$ with respect to the diagonal one $\Delta(t)$. When $\Delta(t) \gg 4E\dot{\theta}_m(t)$, the instantaneous mass eigenstates, ν_i^m , behave approximately as energy eigenstates and they do not mix in the evolution. This is the *adiabatic* transition approximation. From the definition of θ_m in Eq. (60) we find that the adiabaticity condition can be expressed in terms of the adiabaticity parameter Q as

$$\frac{Q}{2} \equiv \frac{\Delta(t)}{4E\dot{\theta}_m(t)} = \frac{\Delta(t)^3}{2EA\Delta m^2 \sin 2\theta} \left| \frac{A}{\dot{A}} \right| \gg 1. \quad (69)$$

Since for small mixing angles the maximum of $\dot{\theta}_m$ occurs at the resonance point (as seen in Fig. 3), the strongest adiabaticity condition is obtained when Eq. (69) is evaluated at the resonance

$$Q = \frac{2\pi\delta r_R}{L_R^{osc}}, \quad (70)$$

where we used the definitions of A_R and δr_R in Eqs. (62) and (65). Written in this form, we see that the adiabaticity condition, $Q \gg 1$, implies that many oscillations take place in the resonant region. Conversely, when $Q \leq 1$ the transition is non-adiabatic.

From the expressions above we see that, for example, the amplitude of a ν_α produced in matter at t_0 and exiting the matter at $t > t_0$ as ν_β can be written as follows:

$$\begin{aligned} \mathcal{A}(\nu_\alpha \rightarrow \nu_\beta; t) &= \sum_{i,j} \mathcal{A}(\nu_\alpha(t_0) \rightarrow \nu_i(t_0)) \mathcal{A}(\nu_i(t_0) \rightarrow \nu_j(t)) \mathcal{A}(\nu_j(t) \rightarrow \nu_\beta(t)) \\ \mathcal{A}(\nu_\alpha(t_0) \rightarrow \nu_i(t_0)) &= \langle \nu_i(t_0) | \nu_\alpha(t_0) \rangle = U_{\alpha i}^*(\theta_{m,0}) \\ \mathcal{A}(\nu_j(t) \rightarrow \nu_\beta(t)) &= \langle \nu_\beta(t) | \nu_j(t) \rangle = U_{\beta j}(\theta) \end{aligned} \quad (71)$$

where $U_{\alpha i}^*(\theta_{m,0})$ is the (αi) element of the mixing matrix in matter at the production point and $U_{\beta j}(\theta)$ is the (βj) element of the mixing matrix in vacuum.

In the adiabatic approximation the mass eigenstates do not mix so

$$\mathcal{A}(\nu_i(t_0) \rightarrow \nu_j(t)) = \delta_{ij} \langle \nu_i(t) | \nu_i(t_0) \rangle = \delta_{ij} \exp \left\{ i \int_{t_0}^t E_i(t') dt' \right\}. \quad (72)$$

Note that E_i is a function of time because the effective mass μ_i is a function of time,

$$E_i(t') \simeq p + \frac{\mu_i^2(t')}{2p}. \quad (73)$$

Thus the transition probability for the adiabatic case is given by

$$P(\nu_\alpha \rightarrow \nu_\beta; t) = \left| \sum_i U_{\beta i}(\theta) U_{\alpha i}^*(\theta_{m,0}) \exp \left(-\frac{i}{2E} \int_{t_0}^t \mu_i^2(t') dt' \right) \right|^2. \quad (74)$$

For the case of two-neutrino mixing Eq. (74) for $\alpha = \beta$ takes the form

$$P(\nu_\alpha \rightarrow \nu_\alpha; t) = \cos^2 \theta_{m,0} \cos^2 \theta + \sin^2 \theta_{m,0} \sin^2 \theta + \frac{1}{2} \sin 2\theta_{m,0} \sin 2\theta \cos \left(\frac{\delta(t)}{2E} \right), \quad (75)$$

where

$$\delta(t) = \int_{t_0}^t \Delta(t') dt' = \int_{t_0}^t \sqrt{(\Delta m^2 \cos 2\theta - A(t'))^2 + (\Delta m^2 \sin 2\theta)^2} dt',$$

which, in general, has to be evaluated numerically. There are some analytic approximations for specific forms of $A(t')$: exponential, linear ... (see, for instance, Ref. [36]). For $\delta(t) \gg E$ the last term in Eq. (75) is averaged and the survival probability takes the form

$$P(\nu_\alpha \rightarrow \nu_\alpha; t) = \frac{1}{2} [1 + \cos 2\theta_{m,0} \cos 2\theta] \quad (76)$$

The Mikheev-Smirnov-Wolfenstein effect for solar neutrinos

The matter effects discussed in the previous section are of special relevance for solar neutrinos. As the Sun produces ν_e 's in its core, here we shall consider the propagation of a $\nu_e - \nu_X$ neutrino system (X is some superposition of μ and τ , which is arbitrary because ν_μ and ν_τ have only and equal neutral current interactions) in the matter density of the Sun.

The density of solar matter is a monotonically decreasing function of the distance R from the center of the Sun, and it can be approximated by an exponential for $R < 0.9R_\odot$

$$n_e(R) = n_e(0) \exp(-R/r_0) , \quad (77)$$

with $r_0 = R_\odot/10.54 = 6.6 \times 10^7 \text{ m} = 3.3 \times 10^{14} \text{ eV}^{-1}$.

As mentioned above, the nuclear reactions in the Sun produce electron neutrinos. After crossing the Sun, the composition of the neutrino state exiting the Sun will depend on the relative size of $\Delta m^2 \cos 2\theta$ versus $A_0 = 2 E G_F n_{e,0}$ (here 0 refers to the neutrino production point which is near but not exactly at the center of the Sun, $R = 0$).

If the relevant matter potential at production is well below the resonant value, $A_R = \Delta m^2 \cos 2\theta \gg A_0$, matter effects are negligible. With the characteristic matter density and energy of the solar neutrinos, this condition is fulfilled for values of Δm^2 such that $\Delta m^2/E \gg L_{\text{Sun-Earth}}$. So the propagation occurs as in vacuum with the oscillating phase averaged to 1/2 and the survival probability at the exposed surface of the Earth is

$$P_{ee}(\Delta m^2 \cos 2\theta \gg A_0) = 1 - \frac{1}{2} \sin^2 2\theta > \frac{1}{2} . \quad (78)$$

If the relevant matter potential at production is only slightly below the resonant value, $A_R = \Delta m^2 \cos 2\theta \gtrsim A_0$, the neutrino does not cross a region with resonant density, but matter effects are sizable enough to modify the mixing. The oscillating phase is averaged in the propagation between the Sun and the Earth. This regime is well described by an adiabatic propagation, Eq. (76)

$$P_{ee}(\Delta m^2 \cos 2\theta \gtrsim A_0) = \frac{1}{2} [1 + \cos 2\theta_{m,0} \cos 2\theta] . \quad (79)$$

This expression reflects that an electron neutrino produced at A_0 is an admixture of ν_1 with fraction $P_{e1,0} = \cos^2 \theta_{m,0}$ and ν_2 with fraction $P_{e2,0} = \sin^2 \theta_{m,0}$. On exiting the Sun, ν_1 consists of ν_e with fraction $P_{1e} = \cos^2 \theta$, and ν_2 consists of ν_e with fraction $P_{2e} = \sin^2 \theta$ so $P_{ee} = P_{e1,0}P_{1e} + P_{e2,0}P_{2e} = \cos^2 \theta_{m,0} \cos^2 \theta + \sin^2 \theta_{m,0} \sin^2 \theta$ [37–39], exactly as given in Eq. (79). Since $A_0 < A_R$ the resonance is not crossed so $\cos 2\theta_{m,0}$ has the same sign as $\cos 2\theta$ and still $P_{ee} \geq 1/2$.

Finally, in the case that $A_R = \Delta m^2 \cos 2\theta < A_0$, the neutrino can cross the resonance on its way out. In the convention of $\Delta m^2 > 0$ this occurs if $\cos 2\theta > 0$ ($\theta < \pi/4$). which means that in vacuum ν_e is a combination of ν_1 and ν_2 with larger ν_1 component, while at the production point ν_e is a combination of ν_1^m and ν_2^m with larger ν_2^m component. In particular, if the density at the production point is much higher than the resonant density, $\Delta m^2 \cos 2\theta \ll A_0$,

$$\theta_{m,0} = \frac{\pi}{2} \Rightarrow \cos 2\theta_{m,0} = -1 , \quad (80)$$

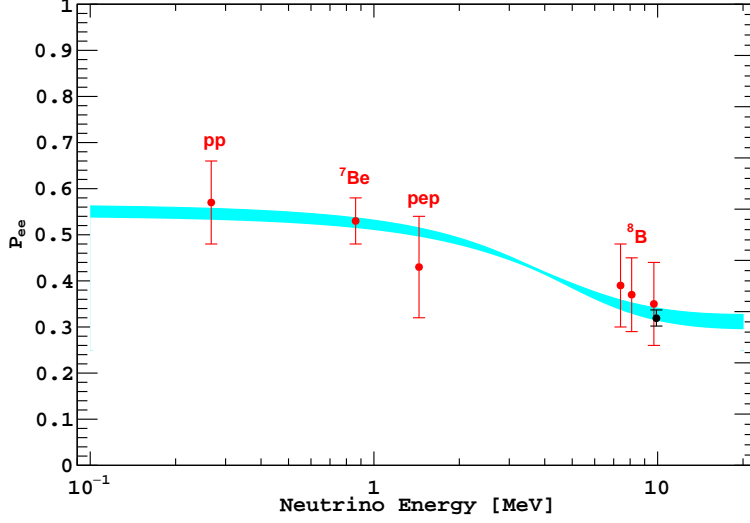


Fig. 4: Electron neutrino survival probability as function of neutrino energy. The points represent, from left to right, the Borexino pp, ${}^7\text{Be}$, pep, and ${}^8\text{B}$ data (red points) and the SNO+SK ${}^8\text{B}$ data (black point). The three Borexino [40] ${}^8\text{B}$ data points correspond, from left to right, to the low-energy (LE) range, LE+HE range, and the high-energy (HE) range. The electron neutrino survival probabilities from experimental points are determined using a high metallicity SSM from Ref. [41]. The error bars represent the $\pm 1\sigma$ experimental + theoretical uncertainties. The curve corresponds to the $\pm 1\sigma$ prediction of the MSW-LMA solution using the parameter values given in Ref. [42]. This figure is taken from Ref. [13] and it was provided by A. Ianni.

and the produced ν_e is purely ν_2^m .

In this regime, the evolution of the neutrino ensemble can be adiabatic or non-adiabatic depending on the particular values of Δm^2 and the mixing angle. We now know that the neutrino masses and mixing happen to be such that the transition is adiabatic in all ranges of solar neutrino energies. Thus the survival probability at the exposed surface of the Earth is given by Eq. (79) but now with mixing angle, Eq. (80), so

$$P_{ee}(\Delta m^2 \cos 2\theta < A_0) = \frac{1}{2} [1 + \cos 2\theta_{m,0} \cos 2\theta] = \sin^2 \theta. \quad (81)$$

So in this case P_{ee} can be much smaller than $1/2$ because $\cos 2\theta_{m,0}$ and $\cos 2\theta$ have opposite signs. This is referred to as the Mikheev-Smirnov-Wolfenstein (MSW) effect [31, 35] which plays a fundamental role in the interpretation of the solar neutrino data.

The resulting energy dependence of the survival probability of solar neutrinos is shown in Fig. 4 (together with a compilation of data from solar experiments). The plotted curve corresponds to $\Delta m^2 \sim 7.5 \times 10^{-5} \text{ eV}^2$ and $\sin^2 \theta \sim 0.3$ (the so-called large mixing angle, LMA, solution). The figure illustrates the regimes described above. For these values of the oscillation parameters, neutrinos with $E \ll 1 \text{ MeV}$ are in the regime with $\Delta m^2 \cos 2\theta \gg A_0$ so the curve represents the value of vacuum averaged survival probability, Eq. (78), and therefore $P_{ee} > 0.5$. For $E > 10 \text{ MeV}$, on the contrary, $\Delta m^2 \cos 2\theta \ll A_0$ and the survival probability is given by Eq. (81), so $P_{ee} = \sin^2 \theta \sim 0.3$. In between, the survival probability is given by Eq. (79) with θ_0 changing rapidly from its vacuum value to the asymptotic matter value, Eq. (80), 90° .

2.3 Experimental evidence of neutrino oscillations

Neutrino flavour transitions have been searched for and observed in a variety of experiments using different neutrino sources and detection techniques. Generically the signatures can be classified in *disap-*

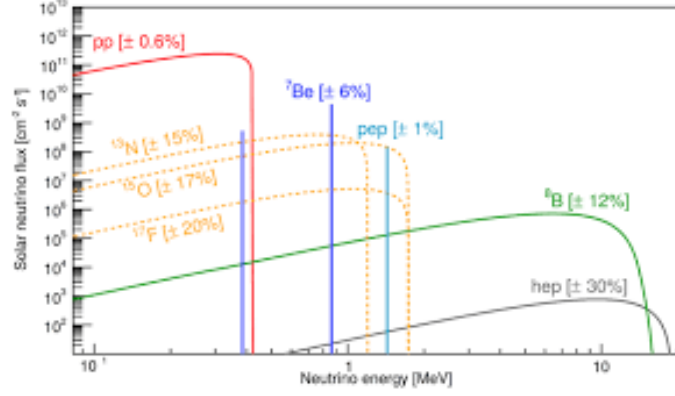


Fig. 5: Neutrino fluxes predicted by the SSM [41] as a function of the neutrino energy.

pearance signals, in which the number of observed neutrino events with the flavour of the original beam is below expectation, and *appearance* signals, in which neutrino events with different flavour than the expected in the beam are observed. Furthermore, to fully establish that the mechanism of flavour transition is that of mass-induced flavour oscillations and to best determine the corresponding mass difference and mixing angles, the experiments study the dependence of the event rates with the distance from the source or with the neutrino energy as well reconstructed as possible.

Solar neutrinos

Solar neutrinos are electron neutrinos produced in the thermonuclear reactions which generate the solar energy. These reactions occur via two main chains, the pp chain and the CNO cycle. There are five reactions which produce ν_e in the pp chain and three in the CNO cycle. Both chains result in the overall fusion of protons into ${}^4\text{He}$:



where the energy released in the reaction, $Q = 4m_p - m_{{}^4\text{He}} - 2m_e \simeq 26 \text{ MeV}$, is mostly radiated through the photons and only a small fraction is carried by the neutrinos, $\langle E_{2\nu_e} \rangle = 0.59 \text{ MeV}$.

In order to precisely determine the rates of the different reactions in the two chains which would give us the final neutrino fluxes and their energy spectrum, a detailed knowledge of the Sun and its evolution is needed. Solar Models (SSM) describe the properties of the Sun and its evolution after entering the main sequence. The models are based on a set of observational parameters and on several basic assumptions: spherical symmetry, hydrostatic and thermal equilibrium, equation of state of an ideal gas, and present surface abundances of elements similar to the primordial composition. I show in Fig. 5 the energy spectrum of the neutrino fluxes from the different reactions together with their present uncertainties as predicted by the SSM in Ref. [41] which is the last version of the Solar Model calculations initiated by Bahcall *et. al* [43]. It is customary to refer to the neutrino fluxes by the corresponding source reaction, so, for instance, the neutrinos produced from ${}^8\text{B}$ decay are called ${}^8\text{B}$ neutrinos.

Solar neutrinos were observed for the first time in 1968 in the Chlorine experiment located in the Homestake mine [44]. Since then they have been detected in a variety of experiments. They can generically be classified as:

- *Radiochemical* detectors, which detect solar ν_e 's by capture in some inverse β decay reaction which leaves as signal the daughter nucleus which are recounted every certain period of time.
 - Chlorine in which ν_e 's are captured via ${}^{37}\text{Cl} (\nu, e^-) {}^{37}\text{Ar}$. The energy threshold for this reaction is 0.814 MeV, so the relevant fluxes are the ${}^7\text{Be}$ and ${}^8\text{B}$ neutrinos. For the SSM fluxes, 78% of the expected number of events are due to ${}^8\text{B}$ neutrinos while 13% arise from

- ${}^7\text{Be}$ neutrinos. The average ν_e event rate measured during the more than 20 years of operation was $\sim 30\%$ of that expected in the SSM [45].
- Gallium experiments: SAGE [46] and GALLEX/GNO [47, 48]. In these experiments the solar neutrinos are captured via ${}^{71}\text{Ga}(\nu, e^-){}^{71}\text{Ge}$. The special properties of this target include a low threshold (0.233 MeV) and a strong transition to the ground level of ${}^{71}\text{Ge}$, which gives a large cross section for the lower energy pp neutrinos. According to the SSM, approximately 54% of the events are due to pp neutrinos, while 26% and 11% arise from ${}^7\text{Be}$ and ${}^8\text{B}$ neutrinos, respectively. The average ν_e event rate measured in both experiments is $\sim 55\%$ of that expected in the SSM.
 - *Real time* detectors in which the interaction of the solar neutrino is recorded in real time.
 - Water Cherenkov detectors: Kamiokande [49, 49] and SuperKamiokande (SK) [50, 51]. They are able to detect in real time the electrons which are emitted from the water by the elastic scattering (ES) of the solar neutrinos, $\nu_a + e^- \rightarrow \nu_a + e^-$. The detection threshold is above ~ 5 MeV. This means that these experiments are able to measure only the ${}^8\text{B}$ neutrinos (and the very small hep neutrino flux). They observe a rate of about $\sim 40\%$ of the SSM prediction. Notice that, while the detection process in radiochemical experiments is purely a CC (W -exchange) interaction, the detection ES process goes through both CC NC (Z -exchange) interactions. Consequently, the ES detection process is sensitive to all active neutrino flavors, although ν_e 's (which are the only ones to scatter via W -exchange) give a contribution that is about 6 times larger than that of ν_μ 's or ν_τ 's.
 - SNO: The Sudbury Neutrino Observatory (SNO) is a Cherenkov detector using heavy water D_2O as target. Solar neutrinos can interact in the D_2O of via three different reactions. Electron neutrinos may interact via the CC reaction $\nu_e + d \rightarrow p + p + e^-$, and can be detected above an energy threshold of a few MeV. All active neutrinos ($\nu_a = \nu_e, \nu_\mu, \nu_\tau$) interact via the NC reaction $\nu_a + d \rightarrow n + p + \nu_a$ with an energy threshold of 2.225 MeV. The non-sterile neutrinos can also interact via ES, $\nu_a + e^- \rightarrow \nu_a + e^-$, but with smaller cross section. The comparison of the observed event rates in the different reactions allow to address the flavour dependence of the solar neutrinos arriving at the Earth. The reactions in the Sun only produce ν_e ', however SNO observed rates which could only be understood if other flavours were present, confirming the flavour transition of solar ν_e' .

These real time experiments have provided us also with information on the time, direction and energy for each event. Signatures of neutrino oscillations might include distortion of the recoil electron energy spectrum, difference between the night-time solar neutrino flux and the day-time flux, or a seasonal variation in the neutrino flux. Observation of these effects were searched for and generically no significant energy or time dependence of the event rates beyond the expected ones in the SSM was observed.

With all the data collected in these experiments it was established that solar neutrinos undergo flavour transitions and they have to be due to the MSW effect in the Sun matter in the adiabatic regime, the so-called Large Mixing Angle (LMA) solution. In Fig. 6 I show the region of masses and mixing which better describe the bulk of solar neutrino data when interpreted in terms of mixing between 2ν states. As seen from the figure these results determine a non-zero $\Delta m^2 \sim \mathcal{O}(10^{-5}) \text{ eV}^2$ and a mixing angle $\sim 32^\circ$.

- Borexino employs a liquid scintillator that produces sufficient light to observe low energy neutrino events via elastic scattering by electrons. The reaction is sensitive to all neutrino flavors by the neutral current interaction, but the cross section for ν_e is larger due to the combination of charged and neutral currents. It has a much lower threshold and better energy resolution than Cherenkov detectors which allows for detail determination of the observed spectrum rates and disentangling the different components once the oscillation parameters are known [40]. A compilation of their results is shown in Fig. 4.

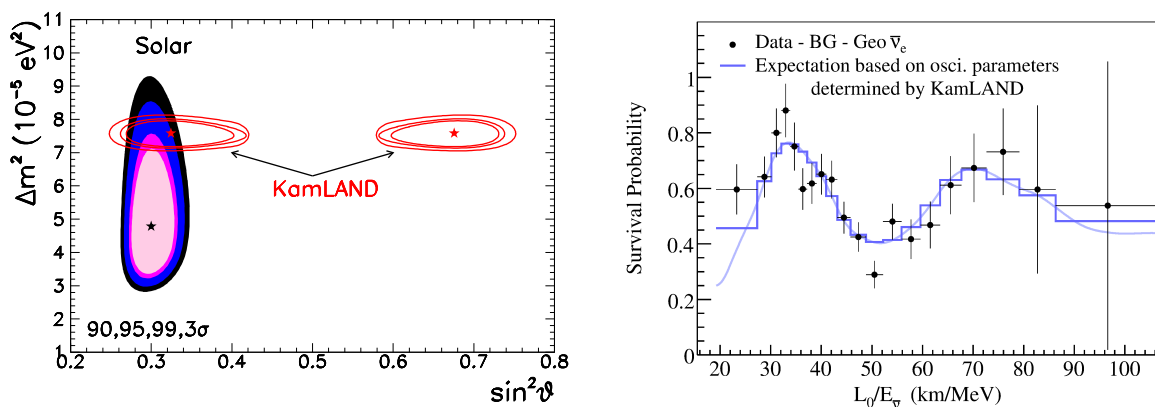


Fig. 6: **Left:** Allowed region of Δm^2 and $\sin^2 \theta$ which better describe the bulk observation of solar data (full regions) and KamLAND spectral data (void regions) at different Confidence Levels (CL) as indicated in the figure when interpreted in terms of flavour oscillations driven by the mixing between 2ν states. **Right:** Ratio of the observed spectrum to the expectation for no-oscillation versus L_0/E for the KamLAND data. $L_0 = 180$ km is the flux-weighted average reactor baseline. The blue line corresponds to the expectation from oscillations of ν_e , taken from Ref. [52].

Reactor neutrinos at long baseline: KamLAND

Neutrino oscillations are also searched for using neutrino beams from nuclear reactors. Nuclear reactors produce $\bar{\nu}_e$ beams with $E_\nu \sim \text{MeV}$. Due to the low energy, e^+ 's are the only charged leptons which can be produced in the $\bar{\nu}_e$ CC interaction. If the $\bar{\nu}_e$ oscillated to another flavor, its CC interaction could not be observed. Therefore oscillation experiments performed at reactors are disappearance experiments. They have the advantage that small values of Δm^2 can be accessed due to the low beam energy. In particular values of Δm^2 as small as $\mathcal{O}(10^{-5}) \text{ eV}^2$ can be accessed in a reactor experiment using a $\mathcal{O}(100)$ km baseline. Pursuing this idea, the KamLAND experiment, a 1000 ton liquid scintillation detector operated in the Kamioka mine in Japan which is located at an average distance of 150–210 km from several Japanese nuclear power stations. The measurement of the energy spectrum of the $\bar{\nu}_e$'s detected in KamLAND [52] is shown in the left panel of Fig. 6 and confirms $\bar{\nu}_e$ oscillations with parameters compatible with those observed in MSW flavour conversion of solar ν_e 's. In the left panel of the same figure I show the parameters region obtained from the fit of KamLAND data in comparison with that from the analysis of solar neutrino data. The figure illustrates the compatibility of the observations. It also illustrates the degeneracy of solutions associated to θ and $\frac{\pi}{2} - \theta$ in 2ν oscillations in vacuum which is broken in the case of flavor transitions in matter as discussed in the previous sections.

Atmospheric neutrinos

Cosmic rays interacting with the nitrogen and oxygen in the Earth's atmosphere at an average height of 15 kilometers produce mostly pions and some kaons that decay into electron and muon neutrinos and anti-neutrinos.

Since ν_e is produced mainly from the decay chain $\pi \rightarrow \mu\nu_\mu$ followed by $\mu \rightarrow e\nu_\mu\nu_e$, one naively expects a 2 : 1 ratio of ν_μ to ν_e . For higher energy events the expected ratio is larger because some of the muons arrive to Earth before they had time to decay. In practice, however, the theoretical calculation of the ratio of muon-like interactions to electron-like interactions in each experiment is more complicated. A set of increasingly more sophisticated calculations of the atmospheric fluxes

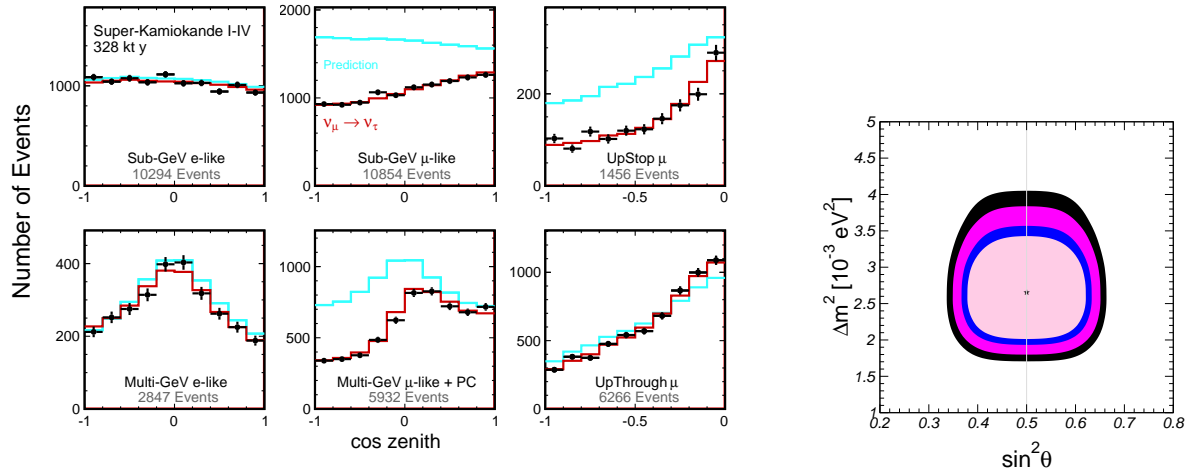


Fig. 7: Left: The zenith angle distribution of different event samples from SK experiment [13]. The points show the data, blue histograms show the non-oscillated expectations and the lines show the best-fit expectations for oscillations. **Right:** The allowed regions (same CL as Fig. 6) of Δm^2 and $\sin^2 \theta$ by the global analysis of SK atmospheric data in the framework of $\nu_\mu \rightarrow \nu_\tau$ vacuum oscillations .

have been performed [53–56] over the years showing that the predicted absolute fluxes of neutrinos produced by cosmic-ray interactions in the atmosphere can vary at the 20% level among the different simulations while their zenith angular dependence, the ratio of neutrinos of different flavor, and the neutrino/antineutrino ratio are much more precisely determined.

Atmospheric neutrinos were first detected in the 1960’s by the underground experiments in South Africa [57] and the Kolar Gold Field experiment in India [58]. A set of modern experiments were proposed and built starting the 1970’s. The original purpose was to search for nucleon decay, for which atmospheric neutrinos constitute a background. But eventually the study of atmospheric neutrino events turned out to be a focus of study following a set of anomalies observed. This culminated with the first evidence of ν_μ oscillation presented by SK. in 1998 [59].

In Fig. 7 [13] I show the data accumulated in SK in its four phases of operation in different event categories and plotted as function of the zenith angle which defines the direction of the observed charged lepton produced in the interaction and which for energies above GeV is very well aligned with the neutrino direction. Upgoing stopping muons arise from neutrinos $E_\nu \sim 10$ GeV, and Upthrough-going muons are originated by neutrinos with energies of the order of hundreds of GeV. Comparing the observed and the expected distributions, we can make the following statements:

- ν_e distributions are well described by the expectations while ν_μ presents a deficit. Thus the atmospheric neutrino deficit is mainly due to disappearance of ν_μ and not the appearance of ν_e .
- The suppression of contained μ -like events is stronger for larger $\cos \theta$, which implies that the deficit grows with the distance traveled by the neutrino from its production point to the detector which ranges from $L \sim 10$ km for $\cos(\text{zenith}) = 1$ to $L \sim 10^4$ km for $\cos(\text{zenith}) = -1$. This effect is more obvious for multi-GeV events because at higher energy the direction of the charged lepton is more aligned with the direction of the neutrino.
- There is very little deficit on the number of through-going muons which implies that at larger energy the neutrino is less likely to disappear.

The simplest and most direct interpretation of the atmospheric neutrino anomaly is that of muon neutrino oscillations $\nu_\mu \rightarrow \nu_\tau$ with parameters as shown in the right of Fig. 7 As seen from the figure these results

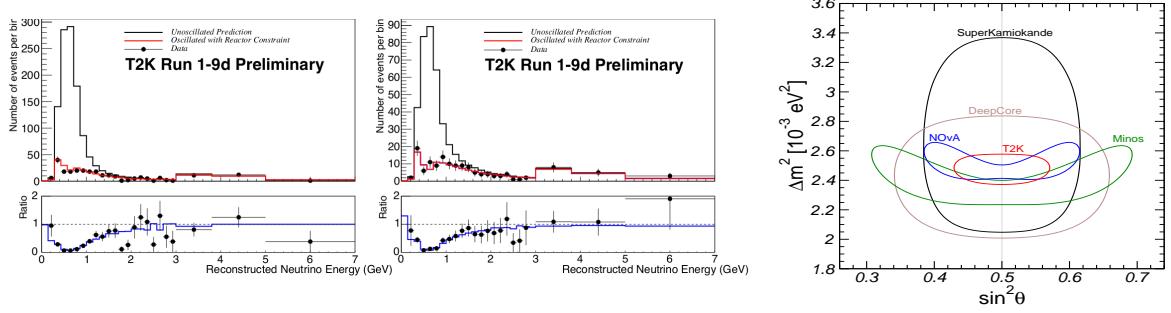


Fig. 8: Spectrum of ν_μ (left) and $\bar{\nu}_\mu$ (center) events observed in T2K. Data points with statistical error bars are shown together with the prediction without (black line) and including (red line) neutrino oscillation. Figure from Ref. [13]. The right panel shows the allowed regions at 95% CL from the analysis of the data in terms of ν_μ disappearance due to oscillations in the 2ν approximation. For comparison the corresponding regions obtained from the analysis of atmospheric neutrino experiments SK and ICECUBE are also shown.

determine a non-zero $\Delta m^2 \sim \mathcal{O}(10^{-3}) \text{ eV}^2$ and a mixing angle $\sim 45^\circ$.

The neutrino telescopes primarily built for the high energy neutrino astronomy such as ANTARES and IceCube can also measure neutrino oscillations with atmospheric neutrinos. IceCube DeepCore [60] provided a precision comparable to the measurements by Super-Kamiokande.

Accelerator neutrinos at long baselines

Conventional neutrino beams from accelerators are mostly produced by π decays (and some K decays), with the pions produced by the scattering of the accelerated protons on a fixed target:

$$\begin{aligned}
 p + \text{target} &\rightarrow \pi^\pm + X \\
 \pi^\pm &\rightarrow \mu^\pm + \nu_\mu(\bar{\nu}_\mu) \\
 \mu^\pm &\rightarrow e^\pm + \nu_e(\bar{\nu}_e) + \bar{\nu}_\mu(\nu_\mu)
 \end{aligned} \tag{83}$$

Thus the beam can contain both μ - and e -neutrinos and antineutrinos. The final composition and energy spectrum of the neutrino beam is determined by selecting the sign of the decaying π and by stopping the produced μ in the beam line. There is an additional contribution to the electron neutrino and antineutrino flux from kaon decay.

Indeed the accelerator neutrino beams are very similar in nature to the atmospheric neutrinos and they can be used to test the observed oscillation signal with a controlled beam. Given the characteristic Δm^2 involved in the interpretation of the atmospheric neutrino signal, the intense neutrino beam from the accelerator must be aimed at a detector located underground at a distance of several hundred kilometers.

The first LBL accelerator experiment was the K2K experiment [61] which run with a baseline of about 235 km from KEK to SK. The MINOS experiment used a beam from Fermilab and a detector in Soudan mine 735 km away [62]. The results from both K2K and MINOS both in the observed deficit of events and in their energy dependence confirmed that accelerator ν_μ oscillate over distances of several hundred kilometers as expected from oscillations with the parameters compatible with those inferred from the atmospheric neutrino data.

In the last decade a second generation of LBL experiments came to operation with the aim at precise determination of the ν_μ disappearance, looking for ν_e appearance and testing the possibility of CP violation. T2K uses the high-intensity beam from the new constructed proton synchrotron J-PARC and the Super-Kamiokande detector at 295 km. The NOvA experiment uses the NuMI beamline with an off-axis configuration. The far detector is located in Minnesota, at 810 km from the source.

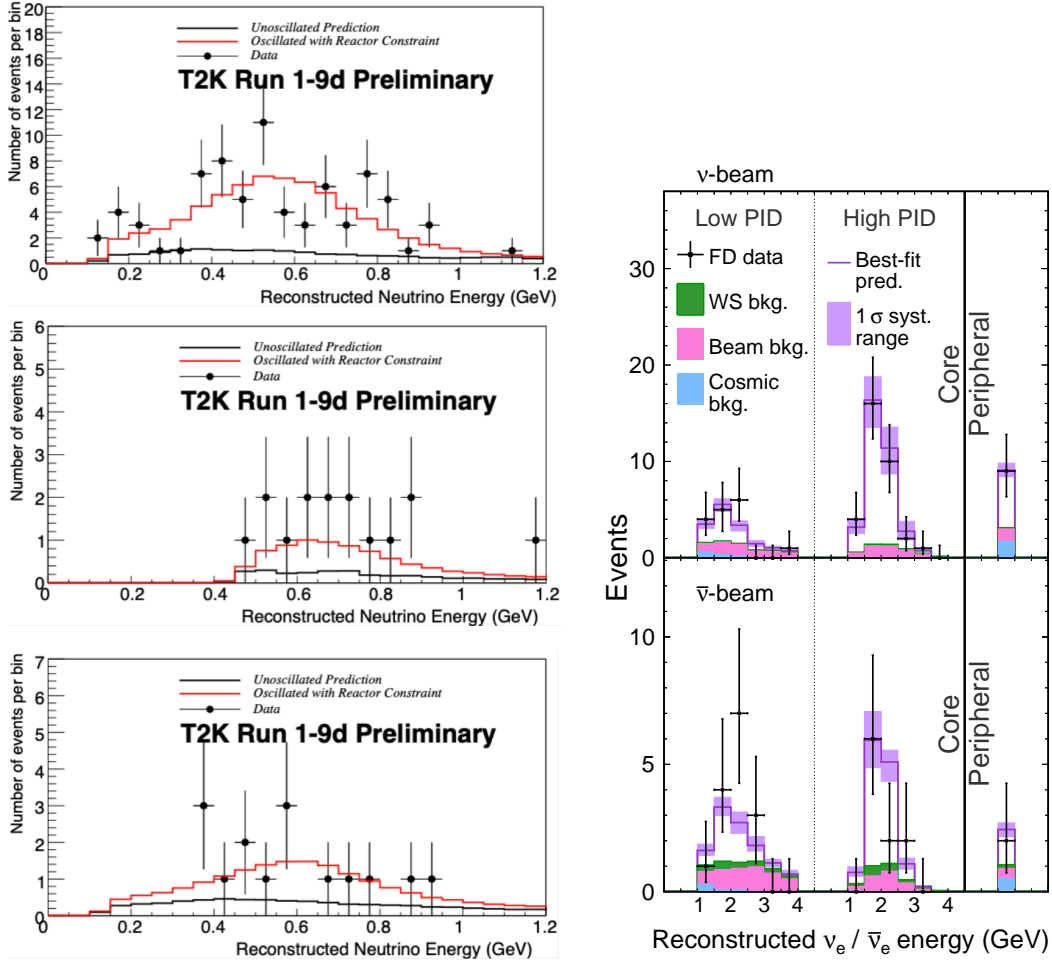


Fig. 9: Spectrum of ν_e and $\bar{\nu}_e$ events observed in T2K [13] (left panels). and NOvA [63].

Both experiments have taken data with ν and with $\bar{\nu}$ beam. Their measured spectrum of μ events allow for precise determination of the same oscillation parameters measured with atmospheric neutrinos. We show in Fig. 8 the observed spectrum of ν_μ and $\bar{\nu}_\mu$ events in T2K together with the allowed regions at 95% CL from the analysis of the data from the different LBL experiments in terms of $\bar{\nu}_\mu$ disappearance due to oscillations in the 2ν approximation compared to those from atmospheric neutrino experiments SK and ICECUBE.

Both experiments have also observed $\nu_\mu \rightarrow \nu_e$ and $\bar{\nu}_\mu \rightarrow \bar{\nu}_e$ transitions. In Fig. 9 I show the spectrum of ν_e and $\bar{\nu}_e$ events in both experiments. If due to oscillations, these results could be explained with a $\Delta m^2 \sim \mathcal{O}(10^{-3})$ eV² is compatible with that inferred from the analysis of $\nu_\mu \rightarrow \nu_\tau$ in atmospheric and LBL neutrinos but with a much smaller mixing angle. Also comparison of the observations in neutrino and antineutrino mode allow for test of CP symmetry. The present situation is that T2K claims a CP violation effect. NOvA indication of leptonic CP violation is less conclusive.

Reactor neutrinos at $\mathcal{O}(\text{km})$ baseline

Over several decades neutrino oscillations were also searched with $\bar{\nu}_e$ fluxes produced by reactors but at baselines of order of kilometer or shorter. Originally they all reported negative results when compared with the expected reactor fluxes obtained with the best calculations of the time. The strongest bounds were established by CHOOZ [64] and Palo Verde [65], which searched for neutrino oscillations in the $\Delta m^2 \sim 10^{-2}$ – 10^{-3} eV² range and set a limit on the corresponding mixing angle $\sin^2 \theta \lesssim 0.025$ at 90%

CL.

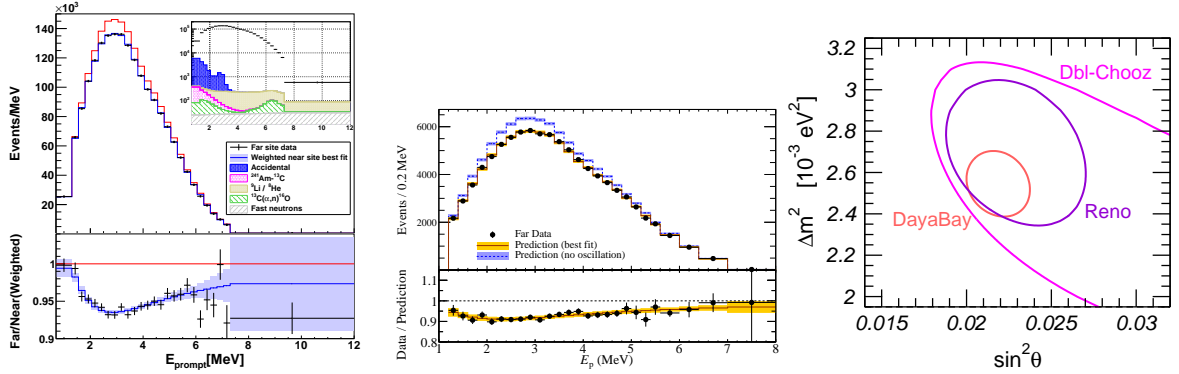


Fig. 10: Energy spectra for prompt events at the far detectors for Daya Bay [66] (left) and RENO [67] (center). The right panel show the allowed regions at 95% CL from the analysis of the data in terms of $\bar{\nu}_e$ disappearance due to oscillations in the 2ν approximation.

This changed over the last decade with three experiments, Double Chooz [68] in France, Daya Bay [66], in China, and RENO [67] in Korea, which to achieve better precision made use of at least two detectors – one near the reactor and other at kilometer distance – allowing to minimize systematics and flux calculation uncertainties. All three report a deficit of events in the far detectors compared with expectation from the observation in the near detector in the absence of oscillations. Furthermore they all measure a distortion of the observed spectrum in the far detectors consistent with oscillations. We show in Fig. 10 the spectrum of events observed in the far detectors in Daya Bay (left) and RENO (center). In the right panel I show the allowed regions at 95% CL from the analysis of this data in terms of $\bar{\nu}_e$ disappearance due to oscillations in the 2ν approximation. As see the $\Delta m^2 \sim \mathcal{O}(10^{-3})$ eV² is compatible with that inferred from the analysis of $\nu_\mu \rightarrow \nu_\tau$ in atmospheric and LBL neutrinos. But the mixing angle $\sim 9^\circ$ is different, and also, unlike in atmospheric and LBL ν_μ disappearance, ν_e 's are involved.

2.4 Summary

Neutrino masses and mixing imply flavour oscillation in vacuum and flavour transitions in matter with a well determined dependence on the distance from the source and the energy of the neutrino. Presently these phenomena have been observed in a variety of experiments. In brief:

- Atmospheric ν_μ and $\bar{\nu}_\mu$ disappear most likely converting to ν_τ and $\bar{\nu}_\tau$. The results show an energy and distance dependence perfectly described by mass-induced oscillations.
- Accelerator ν_μ and $\bar{\nu}_\mu$ disappear over distances of ~ 200 to 800 km. The energy spectrum of the results show a clear oscillatory behaviour also in accordance with mass-induced oscillations with wavelength in agreement with the effect observed in atmospheric neutrinos.
- Accelerator ν_μ and $\bar{\nu}_\mu$ appear as ν_e and $\bar{\nu}_e$ at distances ~ 200 to 800 km.
- Solar ν_e convert to ν_μ and/or ν_τ . The observed energy dependence of the effect is well described by massive neutrino conversion in the Sun matter according to the MSW effect.
- Reactor $\bar{\nu}_e$ disappear over distances of ~ 200 km and ~ 1.5 km with different probabilities. The observed energy spectra show two different mass-induced oscillation wavelengths: at short distances in agreement with the one observed in accelerator ν_μ disappearance, and at long distance compatible with the required parameters for MSW conversion in the Sun.

3 LECTURE III: Implications

3.1 The new minimal Standard Model

From the experimental situation described in the second lecture we conclude that the description of all the data requires an effective model consisting of the SM minimally extended to include neutrino masses with mixing between the three flavour neutrinos of the SM in three distinct mass eigenstates. As mentioned in the first lecture this can be effectively achieved in two different ways:

- Introduce ν_R and impose L conservation so after spontaneous electroweak symmetry breaking

$$\mathcal{L}_D = \mathcal{L}_{SM} - M_\nu \bar{\nu}_L \nu_R + h.c. \quad (84)$$

In this case mass eigenstate neutrinos are Dirac fermions, ie $\nu^C \neq \nu$.

- Construct a mass term only with the SM left-handed neutrinos by allowing L violation

$$\mathcal{L}_M = \mathcal{L}_{SM} - \frac{1}{2} M_\nu \bar{\nu}_L \nu_L^c + h.c. \quad (85)$$

In this case the mass eigenstates are Majorana fermions.

In either case U is a 3×3 matrix but which for Majorana (Dirac) neutrinos depends on six (four) independent parameters: three mixing angles and three (one) phases

$$U = \begin{pmatrix} 1 & 0 & 0 \\ 0 & c_{23} & s_{23} \\ 0 & -s_{23} & c_{23} \end{pmatrix} \cdot \begin{pmatrix} c_{13} & 0 & s_{13} e^{-i\delta_{CP}} \\ 0 & 1 & 0 \\ -s_{13} e^{i\delta_{CP}} & 0 & c_{13} \end{pmatrix} \cdot \begin{pmatrix} c_{21} & s_{12} & 0 \\ -s_{12} & c_{12} & 0 \\ 0 & 0 & 1 \end{pmatrix} \cdot \begin{pmatrix} e^{i\eta_1} & 0 & 0 \\ 0 & e^{i\eta_2} & 0 \\ 0 & 0 & 1 \end{pmatrix}, \quad (86)$$

where $c_{ij} \equiv \cos \theta_{ij}$ and $s_{ij} \equiv \sin \theta_{ij}$. In addition to the Dirac-type phase δ_{CP} , analogous to that of the quark sector, there are two physical phases η_i associated to the Majorana character of neutrinos.

There are several possible conventions for the ranges of the angles and ordering of the states. The community finally agreed to a parametrization of the leptonic mixing matrix as in Eq. (86). The angles θ_{ij} can be taken without loss of generality to lie in the first quadrant, $\theta_{ij} \in [0, \pi/2]$, and the phase $\delta_{CP} \in [0, 2\pi]$. Values of δ_{CP} different from 0 and π imply CP violation in neutrino oscillations in vacuum [69–71]. The Majorana phases η_1 and η_2 play no role in neutrino oscillations [70, 72].

In this convention there are two non-equivalent orderings for the spectrum of neutrino masses:

- Spectrum with Normal Ordering (NO) with $m_1 < m_2 < m_3 \Rightarrow \Delta m_{31,32}^2 > 0$.
- Spectrum Inverted ordering (IO) with $m_3 < m_1 < m_2 \Rightarrow \Delta m_{31,32}^2 < 0$.

Furthermore the data show a hierarchy between the mass splittings, $\Delta m_{21}^2 \ll |\Delta m_{31}^2| \simeq |\Delta m_{32}^2|$. So in total, the 3- ν oscillation analysis of the existing data involves six parameters: 2 mass differences (one of which can be positive or negative), 3 mixing angles, and the CP phase. I summarize in Table 2 the different experiments which dominantly contribute to the present determination of the different parameters in the chosen convention. The table illustrates that the determination of the leptonic parameters requires global analysis of the data from the different experiments. Over the years these analyses have been in the hands of a few phenomenological groups (see for example Refs. [73–76]). In Fig. 11 I show the determination of the six parameters from the updated analysis in Ref. [73]. Defining the 1σ relative precision of the parameter by $2(x^{\text{up}} - x^{\text{low}})/3(x^{\text{up}} + x^{\text{low}})$, where x^{up} (x^{low}) is the upper (lower) bound on a parameter x at the 3σ level, one reads the following 1σ relative precision (marginalizing over ordering) for the better determined parameters:

$$4\% (\sin^2 \theta_{12}), \quad 2.3\% (\sin^2 \theta_{13}), \quad 16\% (\Delta m_{21}^2), \quad 1.3\% (|\Delta m_{3\ell}^2|) \quad (87)$$

The issues which still require clarification are: the mass ordering discrimination, the determination of θ_{23} and the leptonic CP phase δ_{CP} :

Table 2: Experiments contributing to the present determination of the oscillation parameters.

Experiment	Dominant	Important
Solar Experiments	θ_{12}	$\Delta m_{21}^2, \theta_{13}$
Reactor LBL (KamLAND)	Δm_{21}^2	θ_{12}, θ_{13}
Reactor MBL (Daya-Bay, Reno, D-Chooz)	$\theta_{13}, \Delta m_{31,32}^2 $	
Atmospheric Experiments (SK, IC-DC)		$\theta_{23}, \Delta m_{31,32}^2 , \theta_{13}, \delta_{CP}$
Accel LBL $\nu_\mu, \bar{\nu}_\mu$, Disapp (K2K, MINOS, T2K, NO ν A)	$ \Delta m_{31,32}^2 , \theta_{23}$	
Accel LBL $\nu_e, \bar{\nu}_e$ App (MINOS, T2K, NO ν A)	δ_{CP}	θ_{13}, θ_{23}

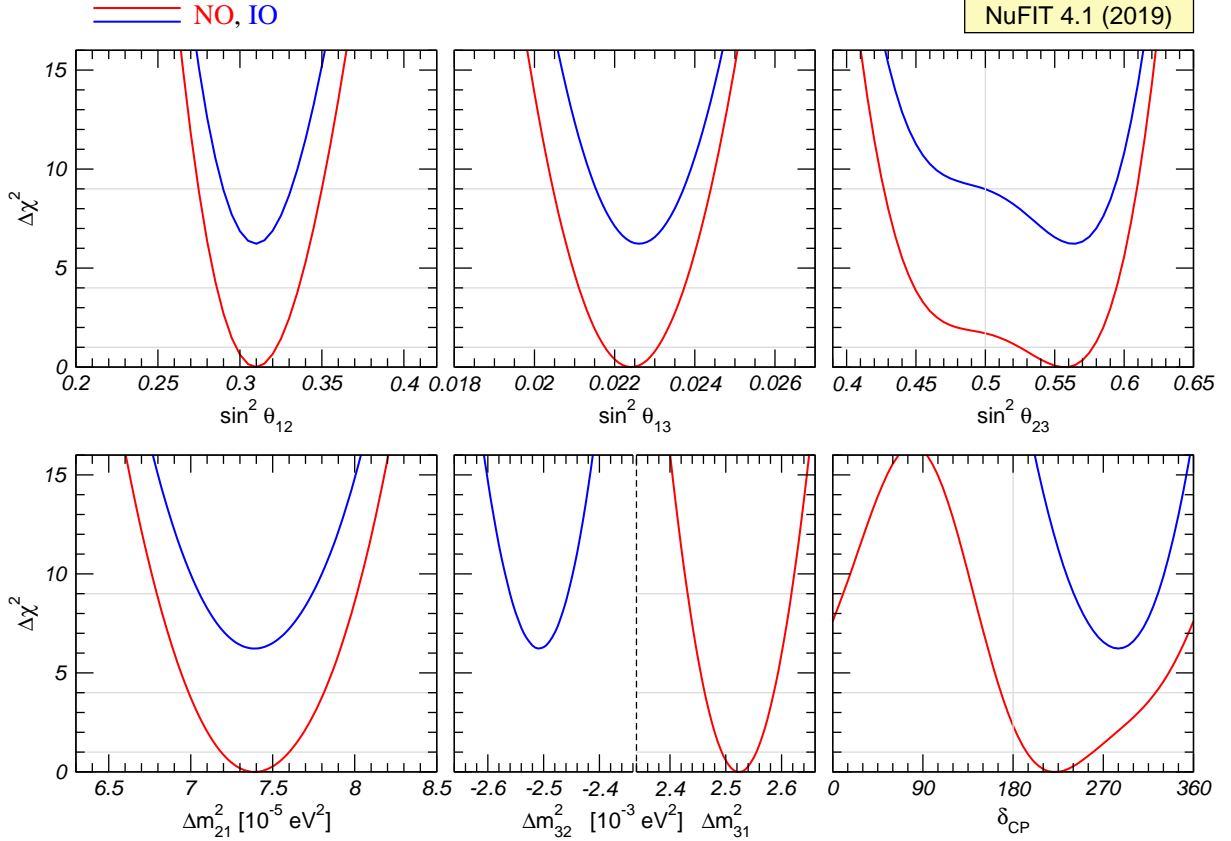


Fig. 11: Global 3ν oscillation analysis. The red (blue) curves are for Normal (Inverted) Ordering. Results for different assumptions concerning the analysis of data from reactor experiments are shown as explained in the text.

- The best fit is for the normal mass ordering. Inverted ordering is disfavoured with a $\Delta\chi^2$ which ranges from slightly above 2σ – driven by the interplay of long-baseline accelerator and short-baseline reactor data – to 3σ when adding the atmospheric χ^2 (not shown in the figure) from Ref. [77].
- The analysis find some preference for the second octant of θ_{23} but with statistical significance still well below 3σ .
- The best fit for the complex phase in NO is at $\delta_{CP} \sim 120^\circ$ but CP conservation (for $\delta_{CP} \sim 180^\circ$) is still allowed at a confidence level (CL) of 1- 2σ . We notice that, at present, the significance of CP violation in the global analysis is reduced with respect to that reported by T2K [78] because NO ν A data does not show a significant indication of CP violation.

These results yield the present determination of the modulus of the leptonic mixing matrix

$$|U|_{3\sigma} = \begin{pmatrix} 0.797 \rightarrow 0.842 & 0.518 \rightarrow 0.585 & 0.143 \rightarrow 0.156 \\ 0.233 \rightarrow 0.495 & 0.448 \rightarrow 0.679 & 0.639 \rightarrow 0.783 \\ 0.287 \rightarrow 0.532 & 0.486 \rightarrow 0.706 & 0.604 \rightarrow 0.754 \end{pmatrix}, \quad (88)$$

which is still much less precisely known than the corresponding quark CKM mixing matrix [14]

$$|V|_{\text{CKM}} = \begin{pmatrix} 0.97427 \pm 0.00015 & 0.22534 \pm 0.0065 & (3.51 \pm 0.15) \times 10^{-3} \\ 0.2252 \pm 0.00065 & 0.97344 \pm 0.00016 & (41.2_{-5}^{+1.1}) \times 10^{-3} \\ (8.67_{-0.31}^{+0.29}) \times 10^{-3} & (40.4_{-0.5}^{+1.1}) \times 10^{-3} & 0.999146_{-0.000046}^{+0.000021} \end{pmatrix}. \quad (89)$$

It is also clear by comparing them that they are very different in structure. Quark CKM matrix is rather *hierarchical* with mixing angles relatively small and smaller for the heavier generation. On the contrary two leptonic mixings are large and even the smaller one, $\theta_{13} \sim 9^\circ$, is not very small.

In the framework of 3ν mixing leptonic CP violation can be quantified in terms of a unique leptonic Jarlskog invariant [79], defined by:

$$\begin{aligned} J_{\text{CP}} &\equiv \text{Im} [U_{\alpha i} U_{\alpha j}^* U_{\beta i}^* U_{\beta j}] \\ &\equiv J_{\text{CP}}^{\text{max}} \sin \delta_{\text{CP}} = \cos \theta_{12} \sin \theta_{12} \cos \theta_{23} \sin \theta_{23} \cos^2 \theta_{13} \sin \theta_{13} \sin \delta_{\text{CP}}. \end{aligned} \quad (90)$$

For example from the analysis in Refs. [73, 74]

$$J_{\text{CP}}^{\text{max}} = 0.03359 \pm 0.0006 (\pm 0.0019), \quad (91)$$

at 1σ (3σ) for both orderings, and the preference of the present data for non-zero δ_{CP} implies a non-zero best fit value $J_{\text{CP}}^{\text{best}} = -0.019$. This can be directly compared with the value of the corresponding invariant in the quark sector $J_{\text{CP}}^{\text{quarks}} = (3.18 \pm 0.15) \times 10^{-5}$ [14].

The status of the determination of leptonic CP violation can also be graphically displayed by projecting the results of the global analysis in terms of leptonic unitarity triangles [80–82]. Since in the analysis U is unitary by construction, any given pair of rows or columns can be used to define a triangle in the complex plane. There a total of six possible triangles corresponding to the unitarity conditions

$$\sum_{i=1,2,3} U_{\alpha i} U_{\beta i}^* = 0 \text{ with } \alpha \neq \beta, \quad \sum_{\alpha=e,\mu,\tau} U_{\alpha i} U_{\alpha j}^* = 0 \text{ with } i \neq j. \quad (92)$$

As illustration we show in Fig. 12 the recasting of the allowed regions of the analysis in Refs. [73, 74] in terms of one leptonic unitarity triangle. We show the triangle corresponding to the unitarity conditions on the first and third columns (after the shown rescaling) which is the equivalent to the one usually shown for the quark sector. In this figure the absence of CP violation would imply a flat triangle, *i.e.*, $\text{Im}(z) = 0$. So the CL at which leptonic CP violation is being observed would be given by the CL at which the region crosses the horizontal axis. For comparison we show in the right panel the present determination of the corresponding unitarity triangle in the quark sector as given in Ref. [14]. Notice that the tiny yellow region in the apex of the triangle in the quark sector is the equivalent to the whole blue region in the leptonic sector.

Projections on neutrino mass scale observables

As discussed in the first lecture, information on the neutrino masses, rather than mass differences, can be extracted from kinematic studies of reactions in which a neutrino or an anti-neutrino is involved. In

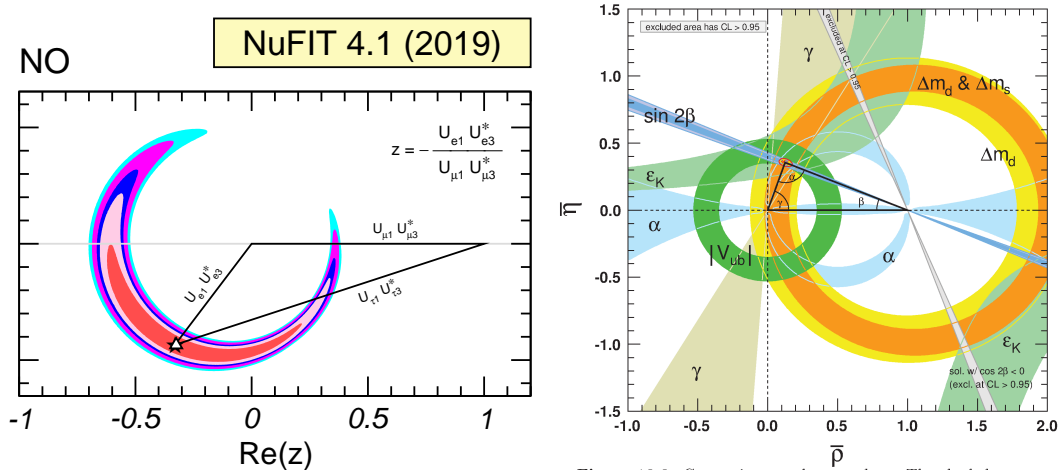


Fig. 12: **Left:** Leptonic unitarity triangle for the first and third columns of the mixing matrix. After scaling and rotating the triangle so that two of its vertices always coincide with $(0, 0)$ and $(1, 0)$ the figure shows the 1σ , 90%, 2σ , 99%, 3σ CL (2 dof) allowed regions of the third vertex for the NO from the analysis in Refs. [73, 74]. **Right:** The corresponding determination of the unitary triangle in the quark sector.

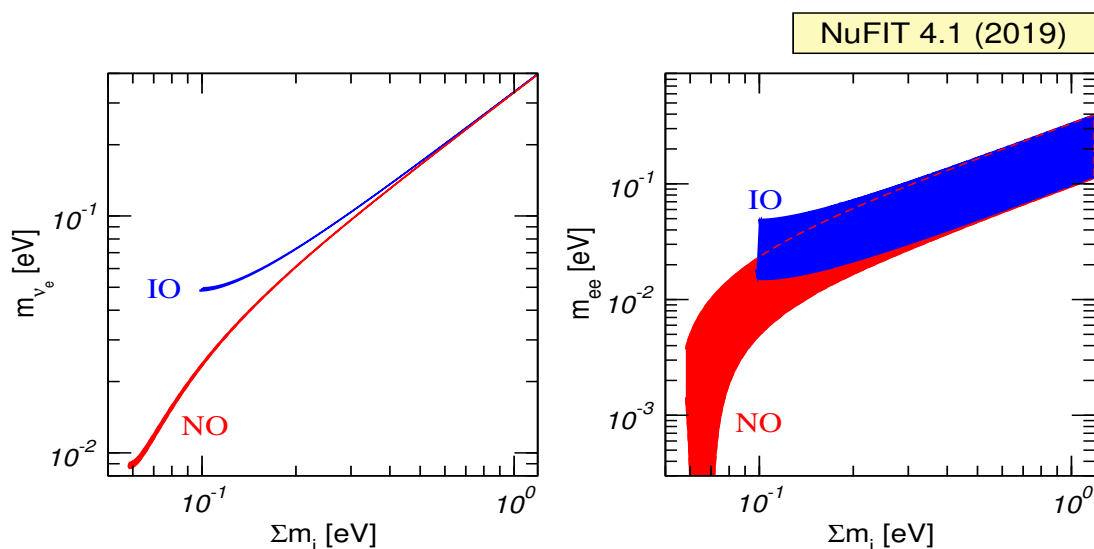


Fig. 13: 95% allowed regions (for 2 dof) in the planes $(m_{\nu_e}^{\text{eff}}, \sum m_{\nu})$ and $(m_{ee}, \sum m_{\nu})$ obtained from projecting the results of the global analysis of oscillation data. The regions are defined with respect to the minimum for each ordering.

the presence of mixing the most relevant constraint comes from the study of the end point of the electron spectrum in Tritium beta decay and for 3ν mixing the $m_{\nu_e}^{\text{eff}}$ introduced in Eq. (33) reads:

$$\begin{aligned}
 m_{\nu_e}^{\text{eff}} &= \frac{\sum_i m_i^2 |U_{ei}|^2}{\sum_i |U_{ei}|^2} = \sum_i m_i^2 |U_{ei}|^2 = c_{13}^2 c_{12}^2 m_1^2 + c_{13}^2 s_{12}^2 m_2^2 + s_{13}^2 m_3^2 \\
 &= \begin{cases} \text{NO:} & m_0^2 + \Delta m_{21}^2 c_{13}^2 s_{12}^2 + \Delta m_{3\ell}^2 s_{13}^2, \\ \text{IO:} & m_0^2 - \Delta m_{21}^2 c_{13}^2 c_{12}^2 - \Delta m_{3\ell}^2 c_{13}^2 \end{cases} \quad (93)
 \end{aligned}$$

where the second equality holds if unitarity is assumed and $m_0 = m_1 (m_3)$ in NO (IO) denotes the lightest neutrino mass.

In what respects the effective Majorana mass of the ν_e which determines the rate of the rate of $0\nu\beta\beta$ decay in the 3ν scenario reads:

$$\begin{aligned}
m_{ee} &= \left| \sum_i m_i U_{ei}^2 \right| = \left| m_1 c_{13}^2 c_{12}^2 e^{i2\alpha_1} + m_2 c_{13}^2 s_{12}^2 e^{i2\alpha_2} + m_3 s_{13}^2 e^{-i2\delta_{\text{CP}}} \right| \\
&= \begin{cases} \text{NO:} & m_0 \left| c_{13}^2 c_{12}^2 e^{i2(\alpha_1 - \delta_{\text{CP}})} + \sqrt{1 + \frac{\Delta m_{21}^2}{m_0^2}} c_{13}^2 s_{12}^2 e^{i2(\alpha_2 - \delta_{\text{CP}})} + \sqrt{1 + \frac{\Delta m_{3\ell}^2}{m_0^2}} s_{13}^2 \right| \\ \text{IO:} & m_0 \left| \sqrt{1 - \frac{\Delta m_{3\ell}^2 + \Delta m_{21}^2}{m_0^2}} c_{13}^2 c_{12}^2 e^{i2(\alpha_1 - \delta_{\text{CP}})} + \sqrt{1 - \frac{\Delta m_{3\ell}^2}{m_0^2}} c_{13}^2 s_{12}^2 e^{i2(\alpha_2 - \delta_{\text{CP}})} + s_{13}^2 \right| \end{cases} \quad (94)
\end{aligned}$$

which, unlike Eq. (93), depends also on the CP violating phases. Finally, as discussed in the first lecture, neutrino masses have also interesting cosmological effects and cosmological data mostly give information on the sum of the neutrino masses, $\sum_i m_i$, while they have very little to say on their mixing structure and on the ordering of the mass states.

Correlated information on these three probes of the neutrino mass scale can be obtained by mapping the results from the global analysis of oscillations presented previously and from the expressions above one finds that the correlations are different for NO and IO. We show in Fig. 13 the present status of this exercise. Also, the relatively large width of the regions in the right panel are due to the unknown Majorana phases. Thus, in principle, from a positive determination of two of these probes, information can be obtained on the the mass ordering [83, 84] and on the value the Majorana phases.

3.2 Beyond the 3ν paradigm: Light sterile neutrinos

Besides the huge success of three-flavour oscillations described above, there are some anomalies which cannot be explained within the 3ν framework and which might point towards the existence of additional neutrino states with masses at the eV scale. In brief:

- the LSND experiment [85] reported evidence for $\bar{\nu}_\mu \rightarrow \bar{\nu}_e$ transitions with $E/L \sim 1 \text{ eV}^2$, where E and L are the neutrino energy and the distance between source and detector.
- this effect has also been searched for by the MiniBooNE experiment [86], which reports a yet unexplained event excess in the low-energy region of the electron neutrino and anti-neutrino event spectra. No significant excess is found at higher neutrino energies. Interpreting the data in terms of oscillations, parameter values consistent with the ones from LSND are obtained, but the test is not definitive;
- radioactive source experiments at the Gallium solar neutrino experiments both in SAGE and GALLEX/GNO have obtained an event rate which is somewhat lower than expected. If not due to uncertainties in the interaction cross section, this effect can be explained by the hypothesis of ν_e disappearance due to oscillations with $\Delta m^2 \gtrsim 1 \text{ eV}^2$ (“Gallium anomaly”) [87, 88];
- new calculations of the neutrino flux emitted by nuclear reactors [89, 90] predict a neutrino rate which is a few percent higher than observed in short-baseline ($L \lesssim 100 \text{ m}$) reactor experiments. If not due to systematic or theoretical uncertainties, a decrease rate at those distances can be explained by assuming $\bar{\nu}_e$ disappearance due to oscillations with $\Delta m^2 \sim 1 \text{ eV}^2$ (“reactor anomaly”) [91]. This reactor anomaly is under study both by the experimental community – with a set of follow-up measurements performed at SBL both at reactors and accelerators –, and by the theory community for improvements of the reactor flux calculations.

As mentioned in the first lecture, whatever the extension of the SM we want to consider it must contain only three light active neutrinos. Therefore if we need more than three light massive states we must add sterile neutrinos to the particle content of the model.

The most immediate question as these anomalies were reported was whether they could all be consistently described in combination with the rest of the neutrino data – in particular with the negative

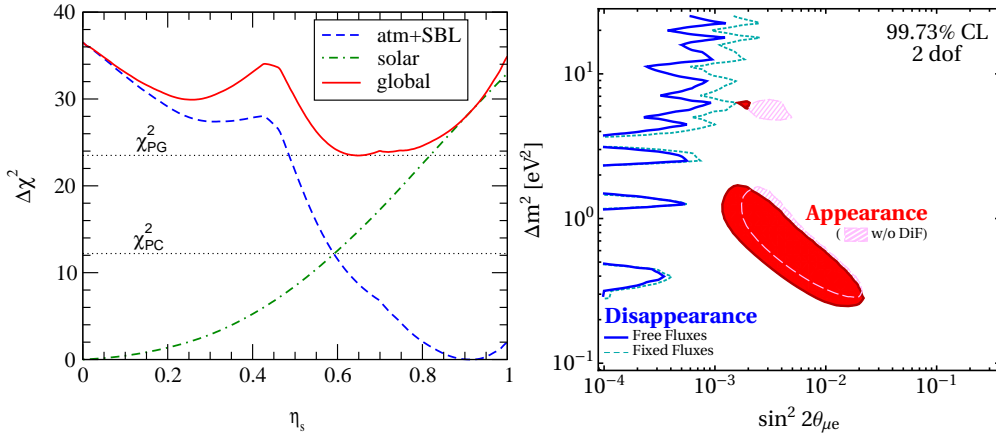


Fig. 14: *Left:* Status of the 2+2 oscillation scenarios from Ref. [93] ($\eta_S = \sum_i |U_{is}|^2$ where i runs over the two massive states mostly relevant for solar neutrino oscillations). In the figure also shown are the values of χ_{PC}^2 and χ_{PG}^2 relevant for parameter consistency test and parameter goodness of fit respectively. *Right:* Present status of 3+1 oscillation scenarios from Ref. [94].

results on disappearance of ν_μ at short distances – if one adds those additional sterile states. Quantitatively one can start by adding a fourth massive neutrino state to the spectrum, and perform a global data analysis to answer this question. Although the answer is always the same the physical reason behind it depends on ordering assumed for the states. In brief, there are six possible four-neutrino schemes which can in principle accommodate the results of solar+KamLAND and atmospheric+LBL neutrino experiments as well as the SBL result. They can be divided in two classes: (2+2) and (3+1). In the (3+1) schemes, there is a group of three close-by neutrino masses (as on the 3ν schemes described in the previous section) that is separated from the fourth one by a gap of the order of 1 eV, which is responsible for the SBL oscillations. In (2+2) schemes, there are two pairs of close masses (one pair responsible for solar results and the other for atmospheric [92]) separated by the $\mathcal{O}(\text{eV})$ gap. The main difference between these two classes is the following: if a (2+2)-spectrum is realized in nature, the transition into the sterile neutrino is a solution of either the solar or the atmospheric neutrino problem, or the sterile neutrino takes part in both. Consequently a (2+2)-spectrum is easier to test because the required mixing of sterile neutrinos in either solar and/or atmospheric oscillations would modify their effective matter potential in the Sun and in the Earth and giving distinctive effects in the solar and/or atmospheric neutrino observables. Those distinctive effects were not observed so oscillations into sterile neutrinos did not describe well either solar or atmospheric data. Consequently as soon as the early 2000's 2+2 spectra could be ruled out already beyond $3\text{--}4\sigma$ as seen in the left panel in Fig.14 taken from Ref. [93]. On the contrary, for a (3+1)-spectrum (and more generally for a $3 + N$ -spectrum with an arbitrary N number of sterile states), the sterile neutrino(s) could be only slightly mixed with the active ones and mainly provide a description of the SBL results. In this case the oscillation probabilities for experiments working at $E/L \sim 1 \text{ eV}^2$ take a simple form:

$$P_{\alpha\alpha} = 1 - \sin^2 2\theta_{\alpha\alpha} \sin^2 \Delta, \quad P_{\mu e} = \sin^2 2\theta_{\mu e} \sin^2 \Delta, \quad (95)$$

where $\Delta \equiv \Delta m_{41}^2 L/4E$ and one can define effective mixing angles

$$\sin^2 2\theta_{\alpha\alpha} \equiv 4|U_{\alpha 4}|^2(1 - |U_{\alpha 4}|^2), \quad \sin^2 2\theta_{\mu e} \equiv 4|U_{\mu 4}|^2|U_{e 4}|^2. \quad (96)$$

In here $\alpha = e, \mu$ and $U_{\alpha 4}$ are the elements of the lepton mixing matrix describing the mixing of the 4th neutrino mass state with the electron and muon flavour. In this scenario there is no sensitivity to CP violation in the the Δ driven oscillations, so the relations above are valid for both neutrinos and

antineutrinos. At linear order in the mixing elements one can derive a relation between the amplitudes of appearance and disappearance probabilities:

$$4 \sin^2 2\theta_{\mu e} \approx \sin^2 2\theta_{ee} \sin^2 2\theta_{\mu\mu}. \quad (97)$$

This relation implies a constraint between the possible results in disappearance and appearance experiments. Consequently it is not trivial to find a consistent description to all the SBL anomalies. Over the years, different groups have performed a variety of such global analysis leading to quantitative different conclusions on the statistical quality of the global fit (see for example Refs. [94–99], see also Refs. [100, 101] for recent reviews on the subject). Generically the results of the global analysis show that there is significant tension between groups of different data sets – in particular between appearance and disappearance results – and Eq. (97) makes it difficult to obtain a good global fit as illustrated in the right panel in Fig. 14 taken from Ref. [94] which concluded that 3+1 scenario is excluded at 4.7σ level.

A straightforward question to ask is whether the situation improves if more neutrino states at the eV scale are introduced. Simplest extension is the introduction of 2 states with eV scale mass splittings, ν_4 and ν_5 . The ordering of the states can be such that Δm_{41}^2 and Δm_{51}^2 are both positive (“3+2”) or one of them is negative (“1+3+1”). From the point of view of the description of the data the most important new qualitative feature is that now non-zero CP violation at $E/L \sim \text{eV}^2$ is possibly observable [97, 102–104]. This allows some additional freedom in fitting neutrino versus anti-neutrino data from LSND and Mini-BooNE together. However, it still holds that a non-zero $\nu_\mu \rightarrow \nu_e$ appearance at SBL necessarily predicts SBL disappearance for both ν_e and ν_μ . So, generically, the tension between appearance and disappearance results remains, though differences in the methodology of statistical quantification of the degree of agreement/disagreement in these scenarios can lead to different conclusions on whether they can provide a successful description of all the data [94, 100, 101].

At present there is an active experimental program to further test these anomalies but the results are still inconclusive.

Cosmological observations can provide complementary information on the number of relativistic neutrino states in thermal equilibrium in the early Universe and on the sum of their masses which sets further constraints on light sterile neutrinos scenarios.

3.3 Beyond the 3ν paradigm: Non-standard interactions

Another extension of the 3ν flavour transitions scenario is that of non-standard neutrino interactions (NSI) with matter. In particular, neutral current NSI’s, which can impact the coherent scattering of neutrinos in matter. They can be parametrized by effective four-fermion operators of the form

$$\mathcal{L}_{\text{NSI}} = -2\sqrt{2}G_F \epsilon_{\alpha\beta}^{fP} (\bar{\nu}_\alpha \gamma^\mu L \nu_\beta) (\bar{f} \gamma_\mu P f), \quad (98)$$

where $f = e, u, d$ is a charged fermion, $P = (L, R)$ and $\epsilon_{\alpha\beta}^{fP}$ are dimensionless parameters encoding the deviation from standard interactions. These operators contribute to the effective matter potential in the Hamiltonian describing the evolution of the neutrino flavour state:

$$H_{\text{mat}} = \sqrt{2}G_F N_e(x) \begin{pmatrix} 1 + \epsilon_{ee} & \epsilon_{e\mu} & \epsilon_{e\tau} \\ \epsilon_{e\mu}^* & \epsilon_{\mu\mu} & \epsilon_{\mu\tau} \\ \epsilon_{e\tau}^* & \epsilon_{\mu\tau}^* & \epsilon_{\tau\tau} \end{pmatrix}, \quad \text{with } \epsilon_{\alpha\beta}(x) = \sum_{f=e,u,d} \frac{N_f(x)}{N_e(x)} \epsilon_{\alpha\beta}^{f,V}, \quad (99)$$

with $N_f(x)$ being the density of fermion f along the neutrino path and $\epsilon_{\alpha\beta}^{f,V} = \epsilon_{\alpha\beta}^{f,L} + \epsilon_{\alpha\beta}^{f,R}$. The “1” in the ee entry in Eq. (99) corresponds to the SM matter potential. Therefore, the effective NSI parameters entering oscillations, $\epsilon_{\alpha\beta}$, may depend on x and will be generally different for neutrinos crossing the Earth or the solar medium and as such can be constrained by the global analysis of neutrino oscillation data.

The task becomes troubled by an intrinsic degeneracy in the Hamiltonian governing neutrino oscillations which is introduced by the NSI-induced matter potential. In general, CPT implies that neutrino evolution is invariant if the relevant Hamiltonian is transformed as $H \rightarrow -H^*$. In vacuum this transformation can be realized by changing the oscillation parameters as

$$\Delta m_{31}^2 \rightarrow -\Delta m_{31}^2 + \Delta m_{21}^2 = -\Delta m_{32}^2, \quad \sin \theta_{12} \leftrightarrow \cos \theta_{12}, \quad \delta_{\text{CP}} \rightarrow \pi - \delta_{\text{CP}}. \quad (100)$$

In the standard 3ν oscillation scenario, this symmetry is broken by the standard matter potential, and this allows for the determination of the octant of θ_{12} and (in principle) of the sign of Δm_{31}^2 . However, in the presence of NSI, the symmetry can be restored if in addition to the transformation Eq. (100), NSI parameters are transformed as

$$(\varepsilon_{ee} - \varepsilon_{\mu\mu}) \rightarrow -(\varepsilon_{ee} - \varepsilon_{\mu\mu}) - 2, \quad (\varepsilon_{\tau\tau} - \varepsilon_{\mu\mu}) \rightarrow -(\varepsilon_{\tau\tau} - \varepsilon_{\mu\mu}), \quad \varepsilon_{\alpha\beta} \rightarrow -\varepsilon_{\alpha\beta}^* \quad (\alpha \neq \beta). \quad (101)$$

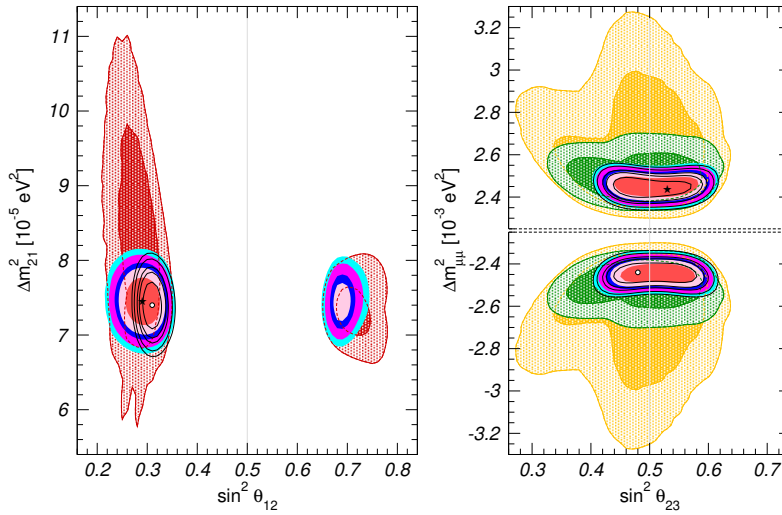


Fig. 15: Two-dimensional projections of the allowed regions onto different vacuum parameters (on the right $\Delta m_{\mu\mu}^2 \simeq \Delta m_{31}^2$) after marginalizing over the matter potential parameters and the not displayed oscillation parameters. The solid colored regions correspond to the global analysis of all oscillation data, and show the 1σ , 90% , 2σ , 99% and 3σ CL allowed regions; the best fit point is marked with a star. The black void regions correspond to the analysis with the standard matter potential (*i.e.*, without NSI) and its best fit point is marked with an empty dot. For comparison, in the left panel we show in red the 90% and 3σ allowed regions including only solar and KamLAND results, while in the right panels we show in green the 90% and 3σ allowed regions excluding solar and KamLAND data, and in yellow the corresponding ones excluding also IceCube and reactor data.

This degeneracy can be seen in Fig. 15 where I show the two-dimensional projections of the allowed regions onto different sets of oscillation parameters from the global analysis in Ref. [105] in the presence of this generalized matter potential, Eq. (99). These regions are obtained after marginalizing over the not displayed vacuum parameters as well as the NSI couplings. For comparison its also shown as black-contour void regions the corresponding results with the standard matter potential, *i.e.*, in the absence of NSI.

From the figure we read the following:

- The determination of the oscillation parameters discussed in the previous section is robust under the presence of NSI as large as allowed by the oscillation data itself with the exception of the octant of θ_{12} . This result relies on the complementarity and synergies between the different data sets, which allows to constrain those regions of the parameter space where cancellations between standard and non-standard effects occur in a particular data set.

- A solution with $\theta_{12} > 45^\circ$ still provides a good fit. This is the *so-called* LMA Dark (LMA-D) solution and it was first found in Ref. [106]. It is a consequence of the intrinsic degeneracy in the Hamiltonian described above. Eq. (100) shows that this degeneracy implies a change in the octant of θ_{12} (as manifest in the LMA-D). As such it cannot be ruled out by oscillation data only. Scattering data, in particular from the finally-observed coherent scattering in nuclei [107] disfavoured it at more than 3σ for NSI coupling neutrinos with either up or down quarks [108]. But it is still allowed for more general NSI couplings [105, 109].

The results of the oscillation analysis show that LMA-D requires large $\varepsilon_{ee} - \varepsilon_{\mu\mu} \sim \mathcal{O}(2)$ which are therefore still allowed. But for all other couplings the same global analysis sets strong constraints on $\varepsilon_{\alpha\beta}$ yielding the most restrictive bounds on the NSI parameters, in particular those involving τ flavour.

3.4 Some implications

The need of new physics and its scale

As we discussed in the first lecture, the SM is a gauge theory based on the gauge symmetry $SU(3)_C \times SU(2)_L \times U(1)_Y$ spontaneously broken to $SU(3)_C \times U(1)_{EM}$ by the vacuum expectation value (VEV), v , of the a Higgs doublet field ϕ with three fermion generations which reside in chiral representations of the gauge group as required by the interactions. No right-handed neutrino is included in the model since neutrinos are neutral.

In the SM, fermion masses arise from the Yukawa interactions, Eq. (8). But no Yukawa interaction can be written that would give mass to the neutrino because no right-handed neutrino field exists in the model. We also argue that neutrino masses could not arise from loop corrections or from non-perturbative effects on the basis of the global symmetries of the model. More precisely, the SM, presents the accidental global symmetry in Eq. (7) which implies that total lepton number $L = L_e + L_\mu + L_\tau$ is a global symmetry of the SM. Therefore any term from loop corrections within this model must conserve total lepton number.

But with the SM particle content the only mass term (that is, the only operator involving a left-handed and a right-handed fermion field) for the neutrino which could be generated would be of the form

$$\left(\bar{L}_{Li} \tilde{\phi} \right) \left(\phi^+ L_{Lj}^C \right) + \text{h.c.}, \quad (102)$$

($L_{Li}^C = C \bar{L}_{Li}^T$) which violates G_{SM}^{global} (in particular it violates total lepton number). Therefore it cannot be generated by SM loop corrections. Also, it cannot be generated by non-perturbative effects.

In other words, the SM predicts that neutrinos are precisely massless and consequently, there is neither mixing nor CP violation in the leptonic sector. Thus the simplest and most straightforward lesson of the experimental evidence for neutrino masses is also the most striking one: *there is new physics beyond the SM*. This has been the first experimental result that is inconsistent with the SM.

Furthermore the determined ranges of neutrino masses and leptonic mixing raise two main questions:

- Why are neutrinos so light?, which is directly related to issue of the origin of neutrino mass.
- Why is lepton mixing so different from quark mixing?, which is related to the flavour puzzle.

A possible way to address these questions is to realize that if the SM is not a complete picture of Nature, then new physics (NP) is expected to appear at some higher energies. In this case the SM is an effective low energy theory valid up to the scale Λ_{NP} which characterizes the NP. In this approach, the gauge group, the fermionic spectrum, and the pattern of spontaneous symmetry breaking are still valid ingredients to describe Nature at energies $E \ll \Lambda_{NP}$. The difference between the SM as a complete description of Nature and as a low energy effective theory is that in the latter case we must consider also non-renormalizable ($\text{dim} > 4$) terms in the Lagrangian whose effect will be suppressed by powers $1/\Lambda_{NP}^{\text{dim}-4}$. In this approach the largest effects at low energy are expected to come from $\text{dim} = 5$ operators

There is a single set of dimension-five terms that is made of SM fields and is consistent with the gauge symmetry given by

$$\mathcal{O}_5 = \frac{c_{5ij}}{2\Lambda_{\text{NP}}} \left(\bar{L}_{Li} \tilde{\phi} \right) \left(\tilde{\phi}^T L_{Lj}^C \right) + \text{h.c.}, \quad (103)$$

which violates total lepton number by two units and leads, upon spontaneous symmetry breaking, to:

$$-L_{M\nu} = \frac{c_{5ij}}{4} \frac{v^2}{\Lambda_{\text{NP}}} \bar{\nu}_i^c \nu_j + \text{h.c.} . \quad (104)$$

Comparing with Eqs. (13) (85) we see that this is a Majorana neutrino mass with:

$$(M_\nu)_{ij} = \frac{c_{5ij}}{2} \frac{v^2}{\Lambda_{\text{NP}}}. \quad (105)$$

Equation (105) arises in a generic extension of the SM which means that neutrino masses are very likely to appear if there is NP. Furthermore comparing Eq. (105) and Eq. (9) we find that the scale of neutrino masses is suppressed by v/Λ_{NP} when compared to the scale of charged fermion masses providing an explanation not only for the existence of neutrino masses but also for their smallness. Finally, Eq. (105) breaks not only total lepton number but also the lepton flavor symmetry $U(1)_e \times U(1)_\mu \times U(1)_\tau$. Therefore we should expect lepton mixing and CP violation.

Given the relation (105), $m_\nu \sim v^2/\Lambda_{\text{NP}}$, it is straightforward to use the measured neutrino masses to estimate the scale of NP that is relevant to their generation. In particular, if there is no quasi-degeneracy in the neutrino masses, the heaviest of the active neutrino masses can be estimated, $m_h = m_3 \sim \sqrt{\Delta m_{31}^2} \approx 0.05$ eV (in the case of inverted hierarchy the implied scale is $m_h = m_2 \sim \sqrt{|\Delta m_{31}^2|} \approx 0.05$ eV). It follows that the scale in the non-renormalizable term (103) is given by

$$\Lambda_{\text{NP}} \sim v^2/m_h \approx 10^{15} \text{ GeV}. \quad (106)$$

We should clarify two points regarding Eq. (106):

1. There could be some level of degeneracy between the neutrino masses that are relevant to the atmospheric neutrino oscillations. In such a case Eq. (106) becomes an upper bound on the scale of NP.
2. It could be that the $c_{5\alpha\beta}$ couplings of Eq. (103) are much smaller than one. In such a case, again, Eq. (106) becomes an upper bound on the scale of NP.

The estimate Eq. (106) is very exciting. First, the upper bound on the scale of NP is well below the Planck scale. This means that there is a new scale in Nature which is intermediate between the two known scales, the Planck scale $m_{\text{Pl}} \sim 10^{19}$ GeV and the electroweak breaking scale, $v \sim 10^2$ GeV. Second, the scale $\Lambda_{\text{NP}} \sim 10^{15}$ GeV is intriguingly close to the scale of gauge coupling unification.

In simple renormalizable realizations of NP this dimension-5 operator can be generated by the tree-level exchange of three types of new particles (see Fig. 16):

- Type-I and Type-III see-saw : One adds at least two fermionic singlets (Type-I) or triplets (Type-III) of mass M and Yukawa couplings λ . The neutrino masses are as Eq. (105) with $\Lambda_{\text{NP}} = M$ and $c_5 \sim \lambda^2$.
- Type-II see-saw: One adds an $SU(2)_L$ Higgs triplet Δ of mass M which couples to the SM $SU(2)_L$ leptons with coupling f , with a neutral component and scalar doublet-triplet mixing μ term in the scalar potential. The neutrino masses are as Eq. (105) with $\Lambda_{\text{NP}} = M^2/\mu$ and $c_5 \sim f$.

Of course, neutrinos could be conventional Dirac particles described as in Eq. (84) and we would be left in the darkness on the reason of the smallness of the neutrino mass.

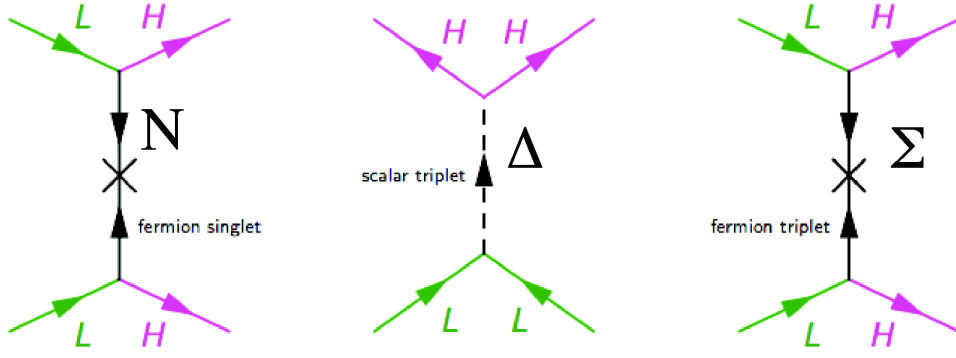


Fig. 16: Tree level diagrams for the Type-I,II and III see-saw, leading to the dim-5 operator for neutrino mass after integrating out the intermediate state

The possibility of leptogenesis

An interesting consequence of neutrinos acquiring their mass via the generic scenario described above is the possibility of explaining the cosmic matter-antimatter asymmetry via the process of leptogenesis [110] in the early Universe.

From what we see and measure, the Universe is made of particles and not of antiparticles. This fact can be quantified in terms of the difference between the density of baryons and antibaryons normalized to the density of photons:

$$Y_B = \frac{n_B - n_{\bar{B}}}{n_\gamma} \sim \frac{n_B}{n_\gamma} \quad (107)$$

From the Big-Bang nucleosynthesis and from the precise data on measurements of the cosmic microwave background, we know that this asymmetry is tiny:

$$Y_B \approx 5 \times 10^{-10} \quad (108)$$

In a seminal paper, Sakharov [111] established the three conditions that any particle physics theory should verify to be able to generate this asymmetry

- Total baryon number B must be violated,
- C and CP must be violated,
- The process which violate these symmetries must occur out of thermal equilibrium.

In principle the SM verifies these conditions because $B + L$ are violated by non-perturbative effects, CP is violated by the CP phase of the CKM quark mixing matrix, and there is departure from thermal equilibrium at the electroweak phase transition provided it is a first order transition. However within the present bounds of the Higgs mass the electroweak phase transition is not strong first order and furthermore the CKM CP violation is too suppressed. As a consequence $Y_{B,SM} \ll 10^{-10}$.

Leptogenesis [110] is the possible origin of such a small asymmetry related to neutrino physics. In a possible realization of leptogenesis, $L \neq 0$ is generated in the Early Universe by the decay of one of the heavy right-handed neutrinos of the type-I see-saw mechanism with CP being violated in the decay. In this case we have:

- Total lepton number is violated by the Majorana mass term of the right-handed neutrinos.
- Due to the interference between the tree-level and one-loop diagrams shown in Fig. 17 the decay rates of the right-handed neutrino into leptons and anti-leptons can be different, so C and CP can be violated

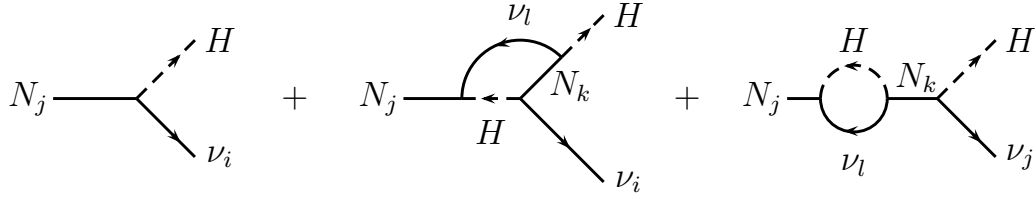


Fig. 17: The tree-level and one-loop diagrams of right-handed neutrino decay into leptons and Higgs.

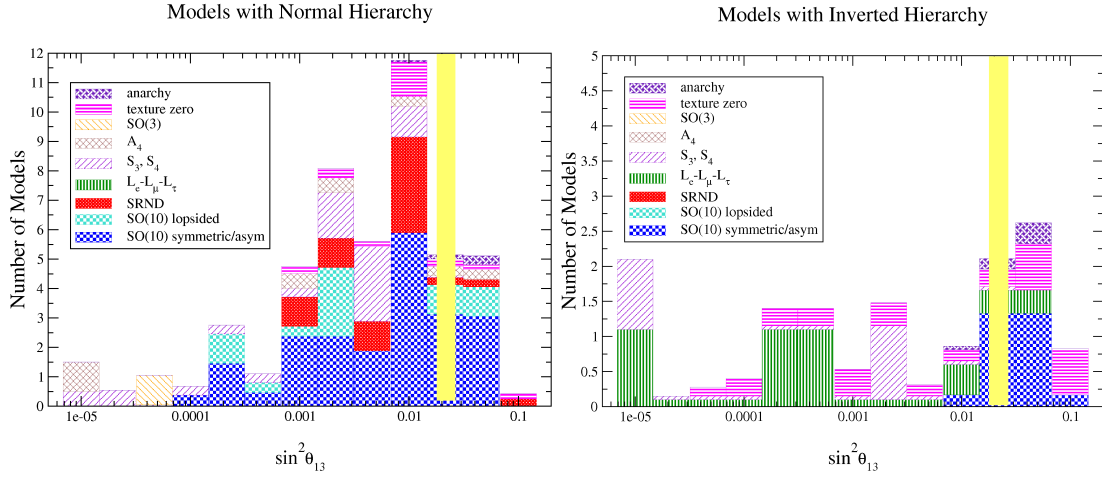


Fig. 18: Compilation in Ref. [113] of the prediction of the value of θ_{13} in several flavour models compared with the present determination.

- The decay can be out of equilibrium if $\Gamma_{\nu_R} \ll$ Universe expansion rate.

Therefore we have all the conditions to generate total lepton number L in the early Universe.

Non perturbative effects known as *sphaleron* [112] processes transform the lepton asymmetry into a baryon asymmetry and below the electroweak phase transition a net baryon asymmetry is generated $\Delta B \simeq -\frac{\Delta L}{2}$ (the exact coefficient relating ΔB to ΔL is model dependent.)

The details of the leptogenesis scenario are model dependent and much work has been done in the framework of specific neutrino models. Generically the resulting asymmetry depends on the size of the CP violating phases, the mass of the lightest heavy neutrino and the light neutrino masses. It has been shown that with the present bounds of the neutrino masses and mixing a right-handed neutrino of about 10^{10} GeV can account for the cosmic baryon asymmetry from its out-of-equilibrium decay.

Implications for flavour models

The relevance of the precise determination of the leptonic mixing matrix to address the flavour puzzle is illustrated in Fig. 18 where I show the compilation in Ref. [113] of the predictions of the expected values of θ_{13} is 63 types of flavour models in 2006. As seen from the figure only about 10% of the models survived the precise determination of θ_{13} in 2012.

Among those which did not survive the test of the precise determination of the mixing parameters were the models predicting bimaximal mixing ($\theta_{12} = \theta_{23} = 45^\circ$, $\theta_{13} = 0$), tri-bimaximal mixing ($\theta_{12} = 35.2^\circ$, $\theta_{23} = 45^\circ$, $\theta_{13} = 0$), and the golden ratio ($\theta_{12} = 31.7^\circ$, $\theta_{23} = 45^\circ$, $\theta_{13} = 0$). Generically these structures appear in models with flavour symmetries with the smallest symmetry groups A_4 , S_4 and A_5 . Consequently either the group has to be enlarged, or corrections to the mixing have to be

obtained from other sectors. Generically these attempts lead to new *sum rules* relating the leptonic flavour parameters among themselves and with those of quarks. Relations which can be testable with enough experimental precision. In this respect the next frontier is the precise determination of the ordering of the states.

Neutrino mass models for collider signatures

One may notice that even in the particularly simple forms of NP of the three type of see-saw realizations represented in Fig. 16, the full theory contains very different high-energy particle contents but they lead to the same low energy operator \mathcal{O}_5 which contains only 9 parameters and that are everything we can measure at neutrino oscillation experiments. This simple example illustrates the limitation of the “bottom-up” approach in deriving model independent implications of the presently observed neutrino masses and mixing. This is the challenge of performing measurements at a much lower scale than that of the NP.

Alternatively one can go “top-down” by studying the low energy effective neutrino masses and mixing induced by specific high energy models as sketched in the discussion about flavour models above.

The bottom line of this discussion is that in order to advance further in the understanding of the dynamics underlying neutrino masses in a model independent approach we need more (and more precise) data. Furthermore synergy among different types of observations such as charge lepton flavour experiments and collider experiments are probably going to be fundamental in this advance. In this respect I will finish by discussing a possible framework in which this connection between neutrino physics and collider signatures arises.

Generically, at low energies the Lagrangian of the full theory can be expanded as

$$\mathcal{L} = \mathcal{L}_{SM} + \frac{c_5}{\Lambda_{LN}} \mathcal{O}_5 + \sum_i \frac{c_{6,i}}{\Lambda_{FL}^2} \mathcal{O}_{6,i} + \dots \quad (109)$$

where \mathcal{O}_5 is Weinberg’s operator responsible for neutrino masses given above, and $\mathcal{O}_{6,i}$ are flavour-changing, but lepton number conserving, dimension-6 operators. In writing Eq. (109) we have explicitly denoted Λ_{LN} as the NP scale for lepton number breaking and Λ_{FL} the NP scale for lepton flavour breaking. In this context attractive testable scenarios are those for which it is possible to relate the mass of the new states $M \sim \Lambda_{FL} \sim \mathcal{O}(\text{TeV})$ but still keep $\Lambda_{LN} \gg \Lambda_{FL}$ to explain the smallness of the neutrino mass.

Furthermore to relate the flavour structure of the signals at collider, or low energy charged lepton flavour experiments with that derived from the neutrino sector one would need some connection between the coefficients c_5 and c_6 . This is precisely provided by the assumption of minimal lepton flavour violation (MLFV) of the NP. Indeed these conditions are automatically fulfilled by the simplest Type-II see-saw model if a light double-triplet mixing μ is assumed. For LHC phenomenology this leads to the interesting possibility of the production of the triplet scalar states with all their decay modes determined by the neutrino mass parameters which has been therefore extensively searched for at LHC. The possibility of constructing and observing MLFV scenarios of Type-I and Type-III see-saws was explored in Refs. [114–116]

References

- [1] E. Fermi, Trends to a theory of beta radiation. (In Italian), *Nuovo Cim.*, **11**(1):19, 1934, doi:10.1007/BF02959820.
- [2] C.L. Cowan *et al.*, Detection of the free neutrino: A confirmation, *Science*, **124**(3212):103–104, 1956, doi:10.1126/science.124.3212.103.
- [3] M. Goldhaber, L. Grodzins, and A.W. Sunyar, Helicity of neutrinos, *Phys. Rev.*, **109**(3):1015–1017, 1958, doi:10.1103/PhysRev.109.1015.

- [4] B. Pontecorvo, Neutrino experiments and the problem of conservation of leptonic charge, *Sov. Phys. JETP*, **26**:984–988, 1968, <https://inspirehep.net/literature/51319>.
- [5] V.N. Gribov and B. Pontecorvo, Neutrino astronomy and lepton charge, *Phys. Lett. B*, **28**(7):493–496, 1969, [doi:10.1016/0370-2693\(69\)90525-5](https://doi.org/10.1016/0370-2693(69)90525-5).
- [6] J.N. Bahcall, *Neutrino astrophysics*, Cambridge Univ. Press, 1989, ISBN:9780521379755.
- [7] R.N. Mohapatra and P.B. Pal, *Massive neutrinos in physics and astrophysics.*, World Scientific, Singapore, 3. ed., 2004, [doi:10.1142/5024](https://doi.org/10.1142/5024).
- [8] C.W. Kim and A. Pevsner, *Neutrinos in physics and astrophysics*, Harwood Academic Publishers, Chur, 1993, ISBN:9783718605675.
- [9] B. Kayser, F. Gibrat-Debu, and F. Perrier, *The physics of massive neutrinos*, World Scientific, Singapore, 1989, [doi:10.1142/0655](https://doi.org/10.1142/0655).
- [10] C. Giunti and C.W. Kim, *Fundamentals of neutrino physics and astrophysics*, Oxford Univ. Press, 2007, [doi:10.1093/acprof:oso/9780198508717.001.0001](https://doi.org/10.1093/acprof:oso/9780198508717.001.0001).
- [11] M.C. Gonzalez-Garcia and Y. Nir, Neutrino masses and mixing: Evidence and implications, *Rev. Mod. Phys.*, **75**(2):345–402, 2003, [doi:10.1103/RevModPhys.75.345](https://doi.org/10.1103/RevModPhys.75.345).
- [12] M.C. Gonzalez-Garcia and M. Maltoni, Phenomenology with massive neutrinos, *Phys. Rept.*, **460**(1-3):1–129, 2008, [doi:10.1016/j.physrep.2007.12.004](https://doi.org/10.1016/j.physrep.2007.12.004).
- [13] M.C. Gonzalez-Garcia and M. Yokoyama, Neutrino masses, mixing, and oscillations, *Prog. Theor. Exp. Phys.*, **2020**(083C01):285–311, 2019, [doi:10.1093/ptep/ptaa104](https://doi.org/10.1093/ptep/ptaa104).
- [14] M. Tanabashi *et al.*, Review of Particle Physics, *Phys. Rev. D*, **98**(3):030001, 2018, [doi:10.1103/PhysRevD.98.030001](https://doi.org/10.1103/PhysRevD.98.030001).
- [15] P. Minkowski, $\mu \rightarrow e\gamma$ at a rate of one out of 10^9 muon decays?, *Phys. Lett. B*, **67**(4):421–428, 1977, [doi:10.1016/0370-2693\(77\)90435-X](https://doi.org/10.1016/0370-2693(77)90435-X).
- [16] P. Ramond, The family group in grand unified theories, in *Int. Symp. Fundamentals of Quantum Theory and Quantum Field Theory, Palm Coast, Florida, 25 February–2 March, 1979*, pp. 265–280, 1979, [arXiv:hep-ph/9809459](https://arxiv.org/abs/hep-ph/9809459).
- [17] M. Gell-Mann, P. Ramond, and R. Slansky, Complex spinors and unified theories, in *Supergravity Workshop Stony Brook, New York, 27–28 September, 1979*, pp. 315–321, 1979, [arXiv:1306.4669](https://arxiv.org/abs/1306.4669).
- [18] T. Yanagida, Horizontal gauge symmetry and masses of neutrinos, in *Proc. Workshop on the Unified Theories and the Baryon Number in the Universe: Tsukuba, Japan, 13–14 February, 1979*, pp. 95–99, 1979, <https://neutrino.kek.jp/seesaw/KEK-79-18-Yanagida.pdf>.
- [19] R.N. Mohapatra and G. Senjanovic, Neutrino mass and spontaneous parity nonconservation, *Phys. Rev. Lett.*, **44**(14):912–915, 1980, [doi:10.1103/PhysRevLett.44.912](https://doi.org/10.1103/PhysRevLett.44.912).
- [20] Z. Maki, M. Nakagawa, and S. Sakata, Remarks on the unified model of elementary particles, *Prog. Theor. Phys.*, **28**(5):870–880, 1962, [doi:10.1143/PTP.28.870](https://doi.org/10.1143/PTP.28.870).
- [21] N. Cabibbo, Unitary symmetry and leptonic decays, *Phys. Rev. Lett.*, **10**(12):531–533, 1963, [doi:10.1103/PhysRevLett.10.531](https://doi.org/10.1103/PhysRevLett.10.531).
- [22] M. Kobayashi and T. Maskawa, CP Violation in the renormalizable theory of weak interaction, *Prog. Theor. Phys.*, **49**(2):652–657, 1973, [doi:10.1143/PTP.49.652](https://doi.org/10.1143/PTP.49.652).
- [23] M. Aker *et al.*, An improved upper limit on the neutrino mass from a direct kinematic method by KATRIN, *Phys.Rev.Lett.*, **123**(22):221802, 2019, [doi:10.1103/PhysRevLett.123.221802](https://doi.org/10.1103/PhysRevLett.123.221802).
- [24] C. Weinheimer *et al.*, The Mainz neutrino mass experiment, *PoS*, **hep2001**:192, 2001, [doi:10.22323/1.007.0192](https://doi.org/10.22323/1.007.0192).
- [25] J. Bonn *et al.*, The Mainz neutrino mass experiment, *Nucl. Phys. B Proc. Suppl.*, **91**(1-3):273–279, 2001, [doi:10.1016/S0920-5632\(00\)00951-8](https://doi.org/10.1016/S0920-5632(00)00951-8).

- [26] V. M. Lobashev *et al.*, Direct search for neutrino mass and anomaly in the tritium beta-spectrum: Status of 'Troitsk neutrino mass' experiment, *Nucl. Phys. B Proc. Suppl.*, **91**(1-3):280–286, 2001, doi:[10.1016/S0920-5632\(00\)00952-X](https://doi.org/10.1016/S0920-5632(00)00952-X).
- [27] J. Schechter and J. W. F. Valle, Neutrinoless double beta decay in SU(2) x U(1) theories, *Phys. Rev. D*, **25**(11):2951, 1982, doi:[10.1103/PhysRevD.25.2951](https://doi.org/10.1103/PhysRevD.25.2951).
- [28] A. Gando *et al.*, Search for Majorana neutrinos near the inverted mass hierarchy region with KamLAND-Zen, *Phys. Rev. Lett.*, **117**(8):082503, 2016, doi:[10.1103/PhysRevLett.117.082503](https://doi.org/10.1103/PhysRevLett.117.082503), Erratum: doi:[10.1103/PhysRevLett.117.109903](https://doi.org/10.1103/PhysRevLett.117.109903).
- [29] J. Engel and J. Menendez, Status and future of nuclear matrix elements for neutrinoless double-beta decay: A review, *Rept. Prog. Phys.*, **80**(4):046301, 2017, doi:[10.1088/1361-6633/aa5bc5](https://doi.org/10.1088/1361-6633/aa5bc5).
- [30] E.Kh. Akhmedov, Quantum mechanics aspects and subtleties of neutrino oscillations, in *Proc. Int. Conf. History of the Neutrino: 1930-2018 Paris, France, 5–7 September, 2018*, 2019, arXiv:[1901.05232](https://arxiv.org/abs/1901.05232).
- [31] L. Wolfenstein, Neutrino oscillations in matter, *Phys. Rev. D*, **17**(9):2369–2374, 1978, doi:[10.1103/PhysRevD.17.2369](https://doi.org/10.1103/PhysRevD.17.2369).
- [32] A. Halprin, Neutrino oscillations in nonuniform matter, *Phys. Rev. D*, **34**(11):3462–3466, 1986, doi:[10.1103/PhysRevD.34.3462](https://doi.org/10.1103/PhysRevD.34.3462).
- [33] P.D. Mannheim, Derivation of the formalism for neutrino matter oscillations from the neutrino relativistic field equations, *Phys. Rev. D*, **37**(7):1935, 1988, doi:[10.1103/PhysRevD.37.1935](https://doi.org/10.1103/PhysRevD.37.1935).
- [34] A.J. Baltz and J. Weneser, Matter oscillations: Neutrino transformation in the sun and regeneration in the earth, *Phys. Rev. D*, **37**(12):3364, 1988, doi:[10.1103/PhysRevD.37.3364](https://doi.org/10.1103/PhysRevD.37.3364).
- [35] S.P. Mikheyev and A. Yu. Smirnov, Resonance amplification of oscillations in matter and spectroscopy of solar neutrinos, *Sov. J. Nucl. Phys.*, **42**:913–917, 1985, <https://inspirehep.net/literature/228623>.
- [36] T.K. Kuo and J. Pantaleone, Neutrino oscillations in matter, *Rev. Mod. Phys.*, **61**(4):937, 1989, doi:[10.1103/RevModPhys.61.937](https://doi.org/10.1103/RevModPhys.61.937).
- [37] S.J. Parke, Nonadiabatic level crossing in resonant neutrino oscillations, *Phys. Rev. Lett.*, **57**(10):1275–1278, 1986, doi:[10.1103/PhysRevLett.57.1275](https://doi.org/10.1103/PhysRevLett.57.1275).
- [38] W.C. Haxton, Adiabatic conversion of solar neutrinos, *Phys. Rev. Lett.*, **57**(10):1271–1274, 1986, doi:[10.1103/PhysRevLett.57.1271](https://doi.org/10.1103/PhysRevLett.57.1271).
- [39] S.T. Petcov, On the nonadiabatic neutrino oscillations in matter, *Phys. Lett. B*, **191**(3):299–303, 1987, doi:[10.1016/0370-2693\(87\)90259-0](https://doi.org/10.1016/0370-2693(87)90259-0).
- [40] M. Agostini *et al.*, Comprehensive measurement of *pp*-chain solar neutrinos, *Nature*, **562**(7728):505–510, 2018, doi:[10.1038/s41586-018-0624-y](https://doi.org/10.1038/s41586-018-0624-y).
- [41] N. Vinyoles *et al.*, A new generation of standard solar models, *Astrophys. J.*, **835**(2):202, 2017, doi:[10.3847/1538-4357/835/2/202](https://doi.org/10.3847/1538-4357/835/2/202).
- [42] J. Bergström *et al.*, Updated determination of the solar neutrino fluxes from solar neutrino data, *JHEP*, **03**:132, 2016, doi:[10.1007/JHEP03\(2016\)132](https://doi.org/10.1007/JHEP03(2016)132).
- [43] J.N. Bahcall, N.A. Bahcall, and G. Shaviv, Present status of the theoretical predictions for the Cl-36 solar neutrino experiment, *Phys. Rev. Lett.*, **20**(21):1209–1212, 1968, doi:[10.1103/PhysRevLett.20.1209](https://doi.org/10.1103/PhysRevLett.20.1209).
- [44] R. Davis, Jr., D.S. Harmer, and K.C. Hoffman, Search for neutrinos from the sun, *Phys. Rev. Lett.*, **20**(21):1205–1209, 1968, doi:[10.1103/PhysRevLett.20.1205](https://doi.org/10.1103/PhysRevLett.20.1205).
- [45] B.T. Cleveland *et al.*, Measurement of the solar electron neutrino flux with the Homestake chlorine detector, *Astrophys. J.*, **496**(1):505–526, 1998, doi:[10.1086/305343](https://doi.org/10.1086/305343).

- [46] J.N. Abdurashitov *et al.*, Solar neutrino flux measurements by the Soviet-American gallium experiment (SAGE) for half the 22 year solar cycle, *J. Exp. Theor. Phys.*, **95**:181–193, 2002, doi:10.1134/1.1506424.
- [47] W. Hampel *et al.*, GALLEX solar neutrino observations: Results for GALLEX IV, *Phys. Lett.*, **B447**:127–133, 1999, doi:10.1016/S0370-2693(98)01579-2.
- [48] M. Altmann *et al.*, Complete results for five years of GNO solar neutrino observations, *Phys. Lett.*, **B616**:174–190, 2005, doi:10.1016/j.physletb.2005.04.068.
- [49] K.S. Hirata *et al.*, Real time, directional measurement of ^8B solar neutrinos in the Kamiokande-II detector, *Phys. Rev.*, **D44**:2241, 1991, doi:10.1103/PhysRevD.44.2241, Erratum: *Phys. Rev.*, **D45**:2170, 1992, doi:10.1103/PhysRevD.45.2170.
- [50] Y. Fukuda *et al.*, Measurements of the solar neutrino flux from Super-Kamiokande's first 300 days, *Phys. Rev. Lett.*, **81**:1158–1162, 1998, doi:10.1103/PhysRevLett.81.1158, Erratum: *Phys. Rev. Lett.*, **81**:4279, 1998, doi:10.1103/PhysRevLett.81.4279.
- [51] S. Fukuda *et al.*, Constraints on neutrino oscillations using 1258 days of Super-Kamiokande solar neutrino data, *Phys. Rev. Lett.*, **86**:5656–5660, 2001, doi:10.1103/PhysRevLett.86.5656.
- [52] S. Abe *et al.*, Precision measurement of neutrino oscillation parameters with KamLAND, *Phys. Rev. Lett.*, **100**:221803, 2008, doi:10.1103/PhysRevLett.100.221803.
- [53] M. Honda *et al.*, Atmospheric neutrino flux calculation using the NRLMSISE-00 atmospheric model, *Phys. Rev.*, **D92**(2):023004, 2015, doi:10.1103/PhysRevD.92.023004.
- [54] G.D. Barr *et al.*, Uncertainties in atmospheric neutrino fluxes, *Phys. Rev.*, **D74**:094009, 2006, doi:10.1103/PhysRevD.74.094009.
- [55] G. Battistoni *et al.*, The FLUKA atmospheric neutrino flux calculation, *Astropart. Phys.*, **19**:269–290, 2003, doi:10.1016/S0927-6505(02)00246-3, Erratum: *Astropart. Phys.*, **19**:291, 2003, doi:10.1016/S0927-6505(03)00107-5.
- [56] J. Evans *et al.*, Uncertainties in atmospheric muon-neutrino fluxes arising from cosmic-ray primaries, *Phys. Rev.*, **D95**(2):023012, 2017, doi:10.1103/PhysRevD.95.023012.
- [57] F. Reines *et al.*, Evidence for high-energy cosmic ray neutrino interactions, *Phys. Rev. Lett.*, **15**:429–433, 1965, doi:10.1103/PhysRevLett.15.429.
- [58] C.V. Achar *et al.*, Detection of muons produced by cosmic ray neutrinos deep underground, *Phys. Lett.*, **18**:196–199, 1965, doi:10.1016/0031-9163(65)90712-2.
- [59] Y. Fukuda *et al.*, Evidence for oscillation of atmospheric neutrinos, *Phys. Rev. Lett.*, **81**:1562–1567, 1998, doi:10.1103/PhysRevLett.81.1562.
- [60] M.G. Aartsen *et al.*, Measurement of atmospheric neutrino oscillations at 6–56 GeV with IceCube DeepCore, *Phys. Rev. Lett.*, **120**(7):071801, 2018, doi:10.1103/PhysRevLett.120.071801.
- [61] S.H. Ahn *et al.*, Detection of accelerator produced neutrinos at a distance of 250 km, *Phys. Lett.*, **B511**:178–184, 2001, doi:10.1016/S0370-2693(01)00647-5.
- [62] D.G. Michael *et al.*, The magnetized steel and scintillator calorimeters of the MINOS experiment, *Nucl. Instrum. Meth.*, **A596**:190–228, 2008, doi:10.1016/j.nima.2008.08.003.
- [63] M.A. Acero *et al.*, First measurement of neutrino oscillation parameters using neutrinos and antineutrinos by NOvA, *Phys. Rev. Lett.*, **123**:151803, 2019, doi:10.1103/PhysRevLett.123.151803.
- [64] M. Apollonio *et al.*, Search for neutrino oscillations on a long baseline at the CHOOZ nuclear power station, *Eur.Phys.J.*, **C27**:331–374, 2003, doi:10.1140/epjc/s2002-01127-9.
- [65] F. Boehm *et al.*, Final results from the Palo Verde neutrino oscillation experiment, *Phys. Rev.*, **D64**:112001, 2001, doi:10.1103/PhysRevD.64.112001.

- [66] D. Adey *et al.*, Measurement of the electron antineutrino oscillation with 1958 days of operation at Daya Bay, *Phys. Rev. Lett.*, **121**(24):241805, 2018, doi:10.1103/PhysRevLett.121.241805.
- [67] G. Bak *et al.*, Measurement of reactor antineutrino oscillation amplitude and frequency at RENO, *Phys. Rev. Lett.*, **121**(20):201801, 2018, doi:10.1103/PhysRevLett.121.201801.
- [68] H. de Kerret *et al.*, Double Chooz θ_{13} measurement via total neutron capture detection, *Nature Phys.*, **16**(5):558–564, 2019, doi:10.1038/s41567-020-0831-y.
- [69] N. Cabibbo, Time reversal violation in neutrino oscillation, *Phys. Lett.*, **72B**:333–335, 1978, doi:10.1016/0370-2693(78)90132-6.
- [70] S.M. Bilenky, J. Hosek, and S.T. Petcov, On oscillations of neutrinos with Dirac and Majorana masses, *Phys. Lett.*, **94B**:495–498, 1980, doi:10.1016/0370-2693(80)90927-2.
- [71] V.D. Barger, K. Whisnant, and R.J.N. Phillips, CP nonconservation in three neutrino oscillations, *Phys. Rev. Lett.*, **45**:2084, 1980, doi:10.1103/PhysRevLett.45.2084.
- [72] P. Langacker *et al.*, Implications of the Mikheev–Smirnov–Wolfenstein (MSW) mechanism of amplification of neutrino oscillations in matter, *Nucl. Phys.*, **B282**:589–609, 1987, doi:10.1016/0550-3213(87)90699-7.
- [73] I. Esteban *et al.*, Global analysis of three-flavour neutrino oscillations: synergies and tensions in the determination of θ_{23} , δ_{CP} , and the mass ordering, *JHEP*, **01**:106, 2019, doi:10.1007/JHEP01(2019)106.
- [74] I. Esteban *et al.*, NuFIT4.1 at NuFit webpage, <http://www.nu-fit.org>, last accessed 22 March 2022.
- [75] F. Capozzi *et al.*, Current unknowns in the three neutrino framework, *Prog. Part. Nucl. Phys.*, **102**:48–72, 2018, doi:10.1016/j.pnpnp.2018.05.005.
- [76] P.F. de Salas *et al.*, Status of neutrino oscillations 2018: 3σ hint for normal mass ordering and improved CP sensitivity, *Phys. Lett.*, **B782**:633–640, 2018, doi:10.1016/j.physletb.2018.06.019.
- [77] K. Abe *et al.*, Atmospheric neutrino oscillation analysis with external constraints in Super-Kamiokande I-IV, *Phys. Rev.*, **D97**(7):072001, 2018, doi:10.1103/PhysRevD.97.072001.
- [78] M. Friend, Updated results from the T2K experiment with 3.13×10^{21} protons on target, January 2019, KEK/J-PARC Physics seminar, 10 January, 2019, <https://t2k.org/docs/talk/335/2019kekseminar>.
- [79] C. Jarlskog, Commutator of the quark mass matrices in the Standard Electroweak Model and a measure of maximal CP nonconservation, *Phys. Rev. Lett.*, **55**:1039, 1985, doi:10.1103/PhysRevLett.55.1039.
- [80] M.C. Gonzalez-Garcia, M. Maltoni, and T. Schwetz, Updated fit to three neutrino mixing: status of leptonic CP violation, *JHEP*, **11**:052, 2014, doi:10.1007/JHEP11(2014)052.
- [81] Y. Farzan and A. Yu. Smirnov, Leptonic unitarity triangle and CP violation, *Phys. Rev.*, **D65**:113001, 2002, doi:10.1103/PhysRevD.65.113001.
- [82] A. Dueck, S.T. Petcov, and W. Rodejohann, On leptonic unitary triangles and boomerangs, *Phys. Rev.*, **D82**:013005, 2010, doi:10.1103/PhysRevD.82.013005.
- [83] G.L. Fogli *et al.*, Observables sensitive to absolute neutrino masses: Constraints and correlations from world neutrino data, *Phys. Rev.*, **D70**:113003, 2004, doi:10.1103/PhysRevD.70.113003.
- [84] S. Pascoli, S. T. Petcov, and T. Schwetz, The absolute neutrino mass scale, neutrino mass spectrum, Majorana CP-violation and neutrinoless double-beta decay, *Nucl. Phys.*, **B734**:24–49, 2006, doi:10.1016/j.nuclphysb.2005.11.003.
- [85] A. Aguilar-Arevalo *et al.*, Evidence for neutrino oscillations from the observation of $\bar{\nu}_e$ appearance in a $\bar{\nu}_\mu$ beam, *Phys. Rev.*, **D64**:112007, 2001, doi:10.1103/PhysRevD.64.112007.
- [86] A.A. Aguilar-Arevalo *et al.*, A combined $\nu_\mu \rightarrow \nu_e$ and $\bar{\nu}_\mu \rightarrow \bar{\nu}_e$ oscillation analysis of the MiniBooNE excesses, *arXiv:1207.4809*, 2012, [arXiv:1207.4809](https://arxiv.org/abs/1207.4809).

- [87] M.A. Acero, C. Giunti, and M. Laveder, Limits on ν_e and $\bar{\nu}_e$ disappearance from gallium and reactor experiments, *Phys. Rev.*, **D78**:073009, 2008, doi:10.1103/PhysRevD.78.073009.
- [88] C. Giunti and M. Laveder, Statistical significance of the gallium anomaly, *Phys. Rev.*, **C83**:065504, 2011, doi:10.1103/PhysRevC.83.065504.
- [89] Th.A. Mueller *et al.*, Improved predictions of reactor antineutrino spectra, *Phys. Rev.*, **C83**:054615, 2011, doi:10.1103/PhysRevC.83.054615.
- [90] P. Huber, Determination of anti-neutrino spectra from nuclear reactors, *Phys. Rev.*, **C84**:024617, 2011, doi:10.1103/PhysRevC.84.024617, Erratum: *Phys. Rev.*, **C85**:029901, 2012, doi:10.1103/PhysRevC.85.029901.
- [91] G. Mention *et al.*, Reactor antineutrino anomaly, *Phys. Rev.*, **D83**:073006, 2011, doi:10.1103/PhysRevD.83.073006.
- [92] J.J. Gomez-Cadenas and M.C. Gonzalez-Garcia, Future ν_τ oscillation experiments and present data, *Z. Phys.*, **C71**:443–454, 1996, doi:10.1007/BF02907002.
- [93] M. Maltoni *et al.*, Ruling out four neutrino oscillation interpretations of the LSND anomaly?, *Nucl. Phys.*, **B643**:321–338, 2002, doi:10.1016/S0550-3213(02)00747-2.
- [94] M. Dentler *et al.*, Updated global analysis of neutrino oscillations in the presence of eV-scale sterile neutrinos, *JHEP*, **08**:010, 2018, doi:10.1007/JHEP08(2018)010.
- [95] C. Giunti and M. Laveder, Status of 3+1 neutrino mixing, *Phys. Rev.*, **D84**:093006, 2011, doi:10.1103/PhysRevD.84.093006.
- [96] J.M. Conrad *et al.*, Sterile neutrino fits to short baseline neutrino oscillation measurements, *Adv. High Energy Phys.*, **2013**:163897, 2013, doi:10.1155/2013/163897.
- [97] J. Kopp *et al.*, Sterile neutrino oscillations: The global picture, *JHEP*, **05**:050, 2013, doi:10.1007/JHEP05(2013)050.
- [98] G.H. Collin *et al.*, First constraints on the complete neutrino mixing matrix with a sterile neutrino, *Phys. Rev. Lett.*, **117**(22):221801, 2016, doi:10.1103/PhysRevLett.117.221801.
- [99] S. Gariazzo *et al.*, Updated global 3+1 analysis of short-baseline neutrino oscillations, *JHEP*, **06**:135, 2017, doi:10.1007/JHEP06(2017)135.
- [100] A. Diaz *et al.*, Where are we with light sterile neutrinos?, *Phys. Rept.*, **884**:1–59, 2019, doi:10.1016/j.physrep.2020.08.005.
- [101] S. Böser *et al.*, Status of light sterile neutrino searches, *Prog. Part. Nucl. Phys.*, **111**:103736, 2020, doi:10.1016/j.pnpnp.2019.103736.
- [102] G. Karagiorgi *et al.*, Leptonic CP violation studies at MiniBooNE in the (3+2) sterile neutrino oscillation hypothesis, *Phys. Rev.*, **D75**:013011, 2007, doi:10.1103/PhysRevD.75.013011, Erratum: *Phys. Rev.*, **D80**:099902, 2009, doi:10.1103/PhysRevD.80.099902.
- [103] M. Maltoni and T. Schwetz, Sterile neutrino oscillations after first MiniBooNE results, *Phys. Rev.*, **D76**:093005, 2007, doi:10.1103/PhysRevD.76.093005.
- [104] C. Giunti and M. Laveder, 3+1 and 3+2 sterile neutrino fits, *Phys. Rev.*, **D84**:073008, 2011, doi:10.1103/PhysRevD.84.073008.
- [105] I. Esteban *et al.*, Updated constraints on non-standard interactions from global analysis of oscillation data, *JHEP*, **08**:180, 2018, doi:10.1007/JHEP08(2018)180.
- [106] O.G. Miranda, M.A. Tortola, and J.W.F. Valle, Are solar neutrino oscillations robust?, *JHEP*, **10**:008, 2006, doi:10.1088/1126-6708/2006/10/008.
- [107] D. Akimov *et al.*, Observation of coherent elastic neutrino-nucleus scattering, *Science*, **357**(6356):1123–1126, 2017, doi:10.1126/science.aao0990.
- [108] P. Coloma *et al.*, COHERENT enlightenment of the neutrino dark side, *Phys. Rev.*, **D96**(11):115007, 2017, doi:10.1103/PhysRevD.96.115007.

- [109] P. Coloma *et al.*, Improved global fit to non-standard neutrino interactions using COHERENT energy and timing data, *JHEP*, **02**:023, 2020, [doi:10.1007/JHEP02\(2020\)023](https://doi.org/10.1007/JHEP02(2020)023), Addendum: *JHEP*, **12**:071, 2020, [doi:10.1007/JHEP12\(2020\)071](https://doi.org/10.1007/JHEP12(2020)071).
- [110] M. Fukugita and T. Yanagida, Baryogenesis without grand unification, *Phys. Lett.*, **B174**:45–47, 1986, [doi:10.1016/0370-2693\(86\)91126-3](https://doi.org/10.1016/0370-2693(86)91126-3).
- [111] A.D. Sakharov, Violation of CP invariance, C asymmetry, and baryon asymmetry of the universe, *Pisma Zh. Eksp. Teor. Fiz.*, **5**:32–35, 1967, English transl. reprinted in *Sov.Phys.Usp.*, **34**(5):392, 1991, [doi:10.1070/PU1991v034n05ABEH002497](https://doi.org/10.1070/PU1991v034n05ABEH002497).
- [112] V.A. Kuzmin, V.A. Rubakov, and M.E. Shaposhnikov, On the anomalous electroweak baryon number nonconservation in the early universe, *Phys. Lett.*, **155B**:36, 1985, [doi:10.1016/0370-2693\(85\)91028-7](https://doi.org/10.1016/0370-2693(85)91028-7).
- [113] C.H. Albright and M.-C. Chen, Model predictions for neutrino oscillation parameters, *Phys. Rev.*, **D74**:113006, 2006, [doi:10.1103/PhysRevD.74.113006](https://doi.org/10.1103/PhysRevD.74.113006).
- [114] M.B. Gavela *et al.*, Minimal flavour seesaw models, *JHEP*, **09**:038, 2009, [doi:10.1088/1126-6708/2009/09/038](https://doi.org/10.1088/1126-6708/2009/09/038).
- [115] O.J.P. Eboli, J. Gonzalez-Fraile, and M.C. Gonzalez-Garcia, Neutrino masses at LHC: Minimal lepton flavour violation in Type-III see-saw, *JHEP*, **12**:009, 2011, [doi:10.1007/JHEP12\(2011\)009](https://doi.org/10.1007/JHEP12(2011)009).
- [116] N.R. Agostinho, O.J.P. Eboli, and M.C. Gonzalez-Garcia, LHC Run I bounds on minimal lepton flavour violation in Type-III see-saw: A case study, *JHEP*, **11**:118, 2017, [doi:10.1007/JHEP11\(2017\)118](https://doi.org/10.1007/JHEP11(2017)118).